



POLITECNICO DI MILANO
DEPARTMENT OF MECHANICAL ENGINEERING
DOCTORAL PROGRAMME IN MECHANICAL ENGINEERING

Constrained optimization of micro injection moulding process

Doctoral Dissertation of:
ing. Gianluca Trotta

Supervisor:
Prof. Quirico Semeraro

Tutor:
Prof. Paolo Emilio Lino Maria Pennacchi

The Chair of the Doctoral Program:
Prof. Andrea Bernasconi

2022 – XXXI

Abstract

The growing industrial interest in micro injection moulding, as leading process able to produce, on large scale, polymeric micro components and micro devices, is pushing towards the definition of a reliable process through the observation of affordable process variables that can be easily measured and optimized.

Part weight in μIM can be considered one of the most significant variables able to provide an easy feedback on the quality of the process.

The work related to the PhD activity is focused on providing an optimization procedure that, starting from a DOE approach, allows to determine a region of the parameters where the performances of the process are optimized (part weight is maximized) subjected to a constraint on the probability of flash formation.

The present approach has a strong industrial relevance in terms of process optimization based on easy to measure quantities while also considering defect formation in the procedure.

The proposed procedure exploits the bootstrap technique and the data depth approach to account for the variability of the process and to build a constrained optimality region.

The selection of the optimal level of the process parameters was carried out using a utility function. The utility function aims at finding a compromise between the maximization of the weight and the minimization of the probability of flash formation. The use of a utility function that correlates two variables of the same process has proved to be fundamental for the construction of the optimality region.

The results evidenced how effective the proposed approach is than the deterministic one. An overimposition of the optimal region for the 5% quantile of utility and median, evidenced the optimality region for micro injection moulding.

The result of this novel approach is a greater variability of the main process parameters, namely T_{melt} and $Phold$, and this means a greater variability of the micro injection moulding process without falling into the risk of producing waste parts.

In Appendix it is reported also a preliminary comparative analysis between simulation and experimentation of the micro injection moulding process. The aim was to assess the simulator's ability to predict the real behavior of the process.

In this preliminary phase of the work it has been identified a regression model with which it is possible to predict in a rather reliable way the set of process and simulation parameters that can minimize the percentage error between the simulation and experimentation weight in absence of flash.

Contents

1. Introduction; 4
2. Context of research; 6
 - 2.1 Macro and Micro injection moulding; 6
 - 2.2 Micro injection moulding: open problems; 10
 - 2.3 Draft resolutions; 12
 - 2.4 References; 13
3. Goal of the PhD activity; 18
 - 3.1 Part weight as the main observed variable; 18
 - 3.1.1 State of the art of part weight; 19
 - 3.2 Constraints related to the part weight; 22
 - 3.3 Description of the original idea; 24
 - 3.4 References; 25
4. Methodologies and tools to build the weight and flash dataset; 31
 - 4.1 Part weight as the main observed variable; 31
 - 4.2 Check of the measurement tool error; 32
 - 4.3 Power analysis and evaluation of the sigma of the process; 34
 - 4.4 Experimental plan; 36
 - 4.5 Dataset definition to identify the part weight and flash models; 38
5. Methodologies and tools to identify the models of part weight and flash constraint to address the optimization problem; 39
 - 5.1 Binary Logistic regression; 39
 - 5.2 Part weight model identification based on reduced dataset; 42
 - 5.3 Summary of the identified models of part weight and flash constraint; 43
6. Optimization problem: procedure, results and discussion; 45
 - 6.1 Binary Logistic regression; 45
 - 6.2 Optimization Procedure; 46
 - 6.3 Results and discussion; 48
 - 6.3.1 Optimal value of part weight under deterministic constraint; 48
 - 6.3.2 Optimal region of part weight under stochastic constraint; 50
 - 6.4 Nomenclature; 54
 - 6.5 References; 55
7. Conclusions; 56
- A1. Part weight comparison between; 58
 - A1.1 Introduction; 58
 - A1.2 Simulator parameters; 59
 - A1.3 Variability range of simulator parameters; 60
 - A1.4 Design of simulated experiments; 62
 - A1.5 Coding of experiments related to flash; 62
 - A1.6 Regression on condition (0 0); 63
 - A1.6.1 Full model; 63
 - A1.6.1 Reduced model for condition (0 0); 64
 - A1.7 Regression analysis on condition (0 0) + (1 0); 65
 - A1.8 Comparison of reduced models; 67; 69
 - A1.9 Conclusions; 68

CHAPTER 1

Introduction

Micro injection moulding (μ IM), among micro manufacturing technologies, is the leading process able to produce, on large scale, polymeric micro components and micro devices. The growing industrial interest in this technology is pushing towards the definition of a reliable process through the observation of affordable process variables that can be easily measured and optimized.

Part weight in μ IM can be considered one of the most significant variables able to provide an easy feedback on the quality of the process. The standard approach to identify combination of parameters that influence the part weight is based on design of experiment, while the desirability function is used to solve multi-optimization problems, such as optimizing both part weight and part weight variability or shrinkage. The process parameters considered in the optimization are mostly similar as well as the material used. The output is a set of processing conditions that ensure the maximization of the performances of the μ IM process.

Optimization techniques are widely used to choose the variable settings that ensure best performances. Usually, the optimization of process parameters results in a selection of only one set of process conditions, such as for RSM, ANOVA, genetic algorithms, etc., and this approach might be too conservative. Boundary conditions might change, and machine performances vary during their lifetime also when they are running in a steady state. The identification of a region of possible optimal values could be more interesting and provide higher flexibility in a manufacturing environment.

Additional complexity is added to the optimization problem when the selection of the optimal process parameters (or the optimal region of the parameters) is subjected to constraints. Constraints might address quality, productivity, or cost issues for example.

Considering only part weight as a performance index is not enough to ensure the production of high-quality part. That is because the maximization of the part weight could imply the presence of other defects, such as flash formation. So, the optimization of the part weight must consider a constraint on the presence of defects. The process parameters that describe the formation of flash in μ IM are the same that define the part weight, so one experimental campaign can be designed to study both part weight and flash formation at the

same time. The results of the experimental campaign can be used to set up a constrained optimization problem to optimize the μIM parameters.

For this reason, the work related to the PhD activity is focused on providing an optimization procedure that, starting from a DOE approach, allows to determine a region of the parameters where the performances of the process are optimized (part weight is maximized) subjected to a constraint on the probability of flash formation.

The present approach has a strong industrial relevance in terms of process optimization based on easy to measure quantities while also considering defect formation in the procedure.

The methodology is significant because it provides not only one combination of parameters but rather a set of optimal conditions that can be used in an industrial environment. Compared to the literature, the problem hereby investigated requires solving an optimization problem where both the objective function and the constraint are estimated from experimental data. This means that both functions are subjected to variability which need to be considered in the procedure.

The proposed procedure exploits the bootstrap technique and the data depth approach to account for the variability of the process and to build a constrained optimality region.

It has been explored also the simulation approach in order to identify a function able to compare the experimental results and the simulated results. Some intrinsic parameters of the simulation tool have been identified and a design of simulated experiments has been implemented, meshing together process parameters and simulation parameters. The purpose is to compare the results with the experiment results and to evaluate if it is possible to obtain a greater control on the simulator in order to minimize the simulation error compared to the experimental data.

datasets has been used to preliminarily test the commercial simulator Autodesk Modflow®. The purpose was to evaluate its prediction capability through the percentage error model.

Context of research

2.1 Macro and Micro injection moulding

Since early 1990s, there has been an increasing demand for compact, integrated and miniaturized products for use in our daily lives as well as for industrial applications.

The various functional micro systems were rapidly widely used in different areas, such as watch and camera industry, printer ink jet, information storage, sensors and transducers, microfluidic system, micro heat exchanger, micro reactor and so on [1]. After impressive development, a new research scientific and engineering area was formed, named as Micro-Electronic-Mechanical systems (MEMs). Especially, in the last twenty years, Micro optical electron system (MOEMS) and Bio- micro electron mechanical system (Bio-MEMS) played important roles in the Information Technology (IT) and Bio-Medical Engineering (BioM) fields [2-6].

The advent of micro system technologies (MST), in addition to microelectronics, has laid the foundations for the development of a new way to think about products and process strategies that are involving in an important way the most strategic fields such as aerospace, automotive and especially biomedical world.

As long as micro manufacturing wasn't considered a mature technology, the first complex and integrated products required well-known macro-fabrication methods, such as forming and machining, and were adapted into micro/meso-scales mainly using intuition and experience.

So, standard injection moulding machines have been adapted to produce such kind of polymeric micro products, but it was immediately clear that this solution was not the right way to support the development of the new area of micro products. The reasons are mainly related to the technological limits of the standard process. Even if the process sequence is somehow the same, from the point of view of the main process phases, reported in Figure 2.1, there is an intrinsic difference related to the whole cycle in terms of time to reach the ejection phase. If we analyze in detail the Figure 2.2, in which the cycle time for standard injection moulding is compared with micro injection moulding one, we can see that the filling time for

micro injection moulding is highly reduced respect to the time for standard injection moulding. [7]

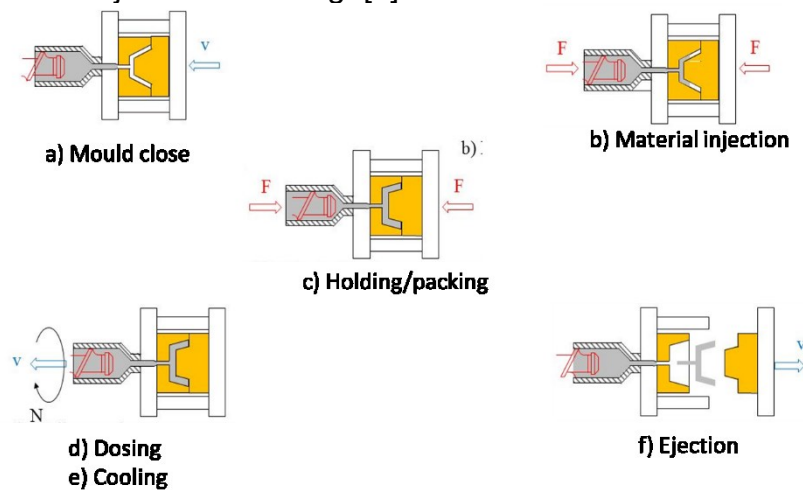


Figure 2.1: Phases of the injection moulding process.

The μ IM process is faster compared to standard injection moulding process, as can be observed by Fig. 2a and 2b. The processing time is shorter to prevent rapid solidification of the molten polymer due to the high heat transfer rate. It can happen that some process steps, such as packing and holding stages, can't concretely become effective because the polymer cool down too fast, as it has been evidenced in Fig. 2b (light blue) where the cooling stage can start already at the end of the fill.

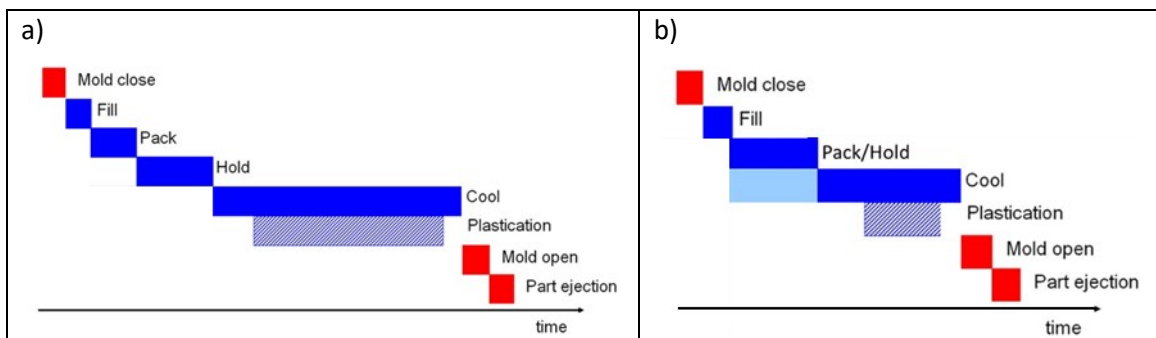


Fig. 2.2: Comparison between: a) typical injection moulding process and b) micro injection moulding production cycle time

These observations can be translated in a completely different kind of machine necessary to operate in these extreme process conditions [7-9]. It is necessary to work at very high speed so that the whole micropart can be completely filled preventing the high cooling rate that can solidificate the part too early [10]. This means also that the advantage of the packing phase, that is usually useful to reduce the shrinkage, can't have effect and consequently the warpage can't be reduced creating problem during demoulding that damages the plastic microparts [11].

The need of high dynamics in such small cavities (Fig. 2.3), however, increase the influence of surface effects, that usually can be neglected in the standard injection moulding, and that becomes, instead, so significant at micro level and must be taken under control

to prevent incomplete filling or defects that can compromise the quality of the final product [12].

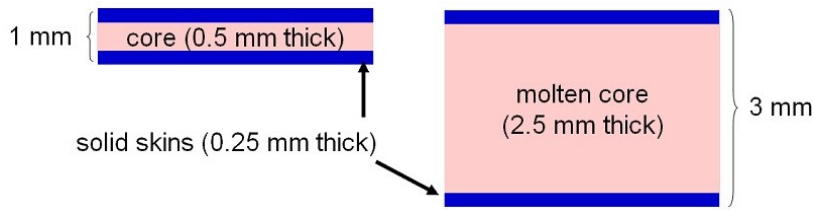


Fig. 2.3: Comparison of cavity thickness between micro and standard injection moulding

Inside the cavity the flow of molten polymer assumes a fountain configuration (Fig. 2.4) and immediately a film of solid material is formed in contact with the surface of the mould, within which the molten material flows. The way the material flows affects the molecular arrangement. In the normal direction to the cavity surface and parallel to the flow direction, gradients of velocity forces arise producing proportional shear forces while shear stresses orient polymer chains in the flow direction.

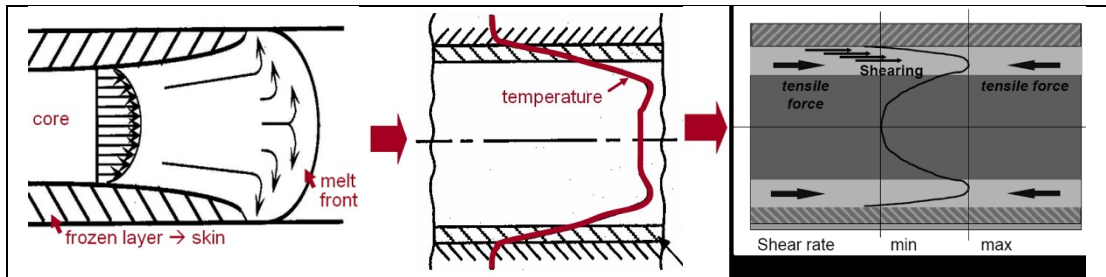


Fig. 2.4: Effect of wall thickness on temperature reduction and on surface tension [13]

If the polymer cools very quickly, as it happens for micro cavities where the temperature of the polymer melt can drop down fast due to reduced cavity dimensions compared to the master mould steel with which the polymer melt is in contact, these orientations freeze influencing the characteristics of the produced part [11].

The quality of the tooling surface, in terms of surface roughness, is another aspect that becomes so important at micro level, as we can see from Fig. 2.5. While for standard cavities the roughness is negligible due to the overall dimension, for micro injection moulding the roughness is proportional to the small cavity thickness and directly impact on the melt flow due to the small layer of material. The viscosity is one of the main aspect directly affected by roughness and tends to increase near to the cavity wall, in particular during the packing phase [14].

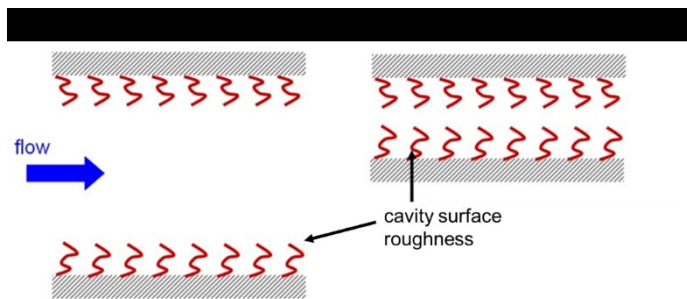


Fig. 2.5: Influence of surface roughness on polymer melting micro cavities

All these surface effects have effect also on the main process parameters of the micro injection moulding process. For the quality of the molded part, for example, it is important that the pressure is as homogeneous as possible at every point of the cavity. The pressure profile of the polymer in the cavity affects the extent of the final shrinkage. So, to reduce deformations, it is essential that the volumetric shrinkage is uniform throughout the cavity and for these reasons the injection pressure necessary to completely fill the micro cavities is higher than standard injection moulding (Fig. 2.6) [11].

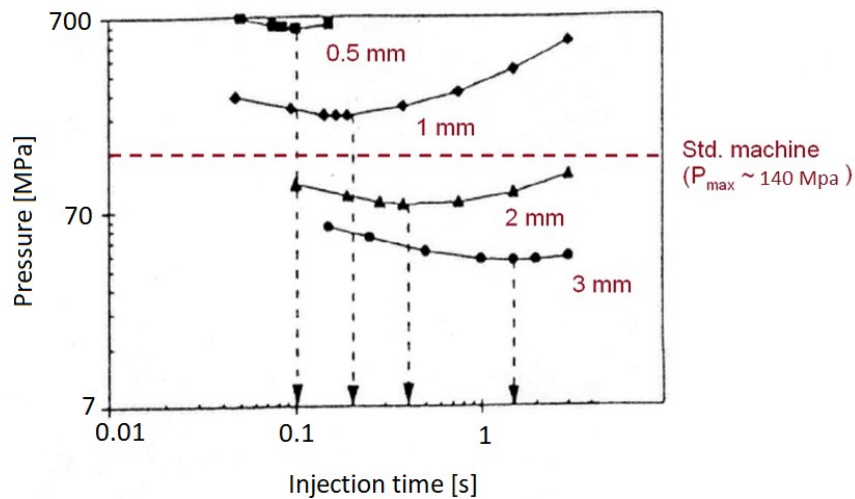


Fig. 2.6: Examples of pressure distribution for different cavity thickness. [13]

Therefore, the high speeds and the high pressures involved require much higher dynamics (Fig. 2.7) but with performance in line with those of classic molding in terms of reliability.

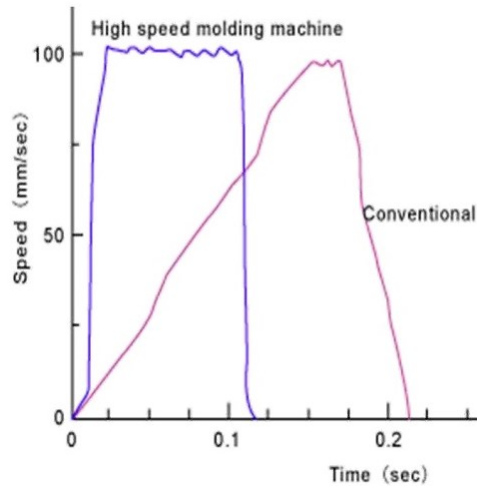


Fig. 2.7: Difference in response time for conventional and high speed molding machine.[13]

2.2 Micro injection moulding: open problems

Micro injection moulding, among all the micro manufacturing technologies, is one of the more complex in terms of number of factors that can concur to the final quality of the product. These factors can be gathered in the following tasks: design, material, process and machine parameters, mould manufacturing strategies and metrological approaches.

The downscale from macro injection moulding to micro injection moulding is not so easy due to the high aspect ratio of the cavities, as seen in the previous section. Some physical aspects that are negligible in injection moulding seems to become so significant in micro injection moulding and the simulation softwares actually available and fully tested for injection moulding present a lot of limitations and are not able to perform good prediction of the behaviour of the polymer flowing through a micro cavity.

Preliminary tests and experiments with conventional injection moulding machines did not respond to the performance and precision requested by such kind of micro products. Huge differences arise comparing the processes from a physical point of view. So, for example, in the micro injection moulding, the layers frozen up to ten times faster than conventional injection moulding [15-17]; the roughness influences the fluidity due to the aspect ratio so tight that the roughness is in the range of aspect ratio too and not in 1% of the thickness as in conventional injection moulding [18-21]. Material database is so poor for such extreme process parameters that the simulation approach fails in some predictions and it is unable to give a quantitative evaluation of the real process [11, 22-23]. Therefore, the development of specific micro injection moulding machines [11, 24] to produce polymeric parts in the range of milligrams ($10 \div 100$ mg) has opened the world to an intensive research activity mainly focused at different steps on the following

topics: the ability to reproduce a micro cavity, the technology required to produce moulds with cavities and inverse features in the range of micrometers, and the opportunity to improve the design using numerical approach [25-27]. These goals also improve research in fields that are essential for the micro injection moulding, such as high precision manufacturing, optical microscopy, roughness measurements, tribology, advanced materials, process optimization and quality control, etc.

The introduced topic is of great interest for the industrial scenario which, after a long period of intense research, is starting to invest more in this technology, thanks to the new markets related, which is now much more mature from the point of view of process knowledge, but that now requires a more important step in the direction of process automation, especially from the point of view of quality control in production. The different approaches to the process emerged from the previous analysis, with respect to the standard process, and the management of components so small or with functionalities at the micrometric level, require important investments for the monitoring of both the process and the product quality.

One of the main challenging points is related to the design limits, and in particular to the simulation tools available on the market, to catch the proper differences with standard injection moulding process [11, 28]. It is clear now that in order to produce such micro components it is necessary to invest towards specific micro injection moulding machines and micro manufacturing technologies able to realize the micro cavities with the precision requested. However, the risk of investment is so high because the cost of the manufacturing process is directly proportional to the complexity and precision requested. Improvements in modelling techniques are much more important now than ever before and the opportunity to obtain models that preserve a stochastic approach, due to the dependence from real process, and that can give suggestions on regions of process efficiency, are essential to make reliable predictions.

Technology suffers of a big lack in the design of components because even if industries are starting to investing in this technology, there are limits in simulation tools that are still not completely able to give a successful response in terms of behaviour of the polymer flow from a quantitative point of view, while they can give good indications on the feasibility of filling the cavity from a qualitative point of view thanks to the calibration guidelines of simulation software developed by researchers in recent years. The main limitations encountered are related to the fact that the rheological data used in current packages are obtained from macroscopic experiments [29] and that a no-slip boundary condition is employed, with the consequence that wall slip cannot be predicted [30-32]. Moreover, surface tension is not taken into account, but it plays a role on the filling of micro-structures [33]. Usually, a constant heat transfer coefficient is assumed, but it cannot describe the flow through micro-channels and its standard value suitable for the simulation of macro-parts differs substantially from values indicated for μ IM [34-37]. Moreover, rheology data provided by the software database are obtained at shear rates and pressures typical of capillary rheometers (i.e., over significantly lower ranges if

compared with those of micro-molding), and therefore they are not directly applicable and not suitable for micro-scale polymer flow applications [29].

Another limitation to the full development of this technology is the difficulty of measuring micro components. In fact, the evaluations on the quality of the component are made off line with very complex devices, such as optical microscopes.

In recent years, some techniques have been introduced, such as fingerprints, also in micro injection moulding, that are specific micro geometries independent from the component to be realized. Its direct observation gives an indication about the quality of the process and of the product. Thanks to a statistical approach, moreover, these fingerprints have been correlated to the process parameters and are able to give indications on which one to operate to improve the quality [60].

The implementation of pressure and temperature monitoring systems in micro cavities has produced better results thanks to the availability on the market of miniaturized sensors capable of simultaneously performing the two measurements. Also in this case the statistical approach allowed to correlate variables, such as pressure and temperature in cavities, to the main process parameters, providing important indications on the behavior of the process. However, this approach is strongly limited to the cavity geometries able to house such sensors in the areas of interest [29].

2.3 Draft resolutions

The study of specific rheological behaviors for high injection speed (up to 500 mm/s) and rapid cooling down have been essential for better reproducing the characteristics of the micro injection molding process [38, 39]. The use of varioterm systems [40-42], vacuum systems [40-46], ultrasound systems [47-50] has been used to improve the viscosity and consequently the flowability in order to reach higher aspect ratio while cavity mould surface roughness [14, 18, 19], heat transfer coefficient [34-35, 51-53], viscosity [38-39, 54-56], wall slip [20, 30, 39], shear stress induced by high shear rates and compressibility of melt flow [34] have been analyzed in detail in order to better define each influence on the replication capability of micro features.

Specialized micro injection molding machine such as Battenfeld, Desmatech and Amburg arised on the market giving the opportunity to work with small polymer quantitates, very high injection speed (injection rate) and high temperatures compared to the conventional injection molding [24]. The use of very precise control units and actuators for plasticizing and filling phases give the opportunity to manage a metering size more precise than before. Within this, the use of cavity pressure/temperature sensors have proven to be important to have a response about the behavior of the melt and to compare the simulation results to improve the reliability and to obtain more information that are difficult to obtain just from the analysis of the process parameters [11]. So, an analytical approach beside simulation and experimentation has been used to identify the phenomenon described above [56].

One of the main goals for micro injection moulding is to improve the flowability so that the micro cavity can be completely filled. An increasing interest in producing polymeric microfluidic devices, such as Lab on a Chip, with mass production technology such as micro injection molding is an essential step in this direction [27, 57]. A deep study of microchannel realized on thin plates seems a priority compared to other issues. The roughness seems really difficult to manage when working with high aspect ratio, such as for microchannel and v-grooves, in particular when approaching with simulation [58]. So rheological models and specific boundary conditions (Cross-WLF for viscosity, Hele-Shaw flow model, Continuity equation, Momentum equation, Energy equation, no slip condition, mold uniform thermal distribution, ecc..) are implemented sometimes in self-made (ad-hoc) simulation programs, with better results but with the difficulty to manage the software itself, largely in commercial simulation tools, but not always with a clear indication of how it is done and how it can be assessed the effectiveness. Later advancements observed in machine development, mold fabrication, temperature control, and process optimization have greatly increased the opportunities of producing smaller and more complex micro products [59]. Research works has focused on the manufacturability of micro products, mainly from the viewpoints of material selection and process control. In recent years, new trends have emerged toward obtaining more accurate and performance-diverse microparts, stepping more closely to the practical applications. The success in characterizing and controlling micro-morphologies and resultant properties has led to increased possibilities of tailoring μ IM products for wider applications. The replication capability of micro injection molding products has become of prior interest due to the increasing demand for polymeric micro devices and micro products and the process starts to be more specialized [24]. Identify response variables that allows to monitor the overall quality of the micro component quickly and effectively is now a crucial requirement. In this perspective, the measurement of the weight of the micro component is certainly one of the most reliable way to evaluate the final quality of the polymeric micro part. The use of DOE approach has become useful in this direction, starting from the Taguchi method of the previous years, when a screening approach among a huge number of parameters has been investigated and then refined with ANOVA to identify the best level set of parameters selected as most influential, up to more refined factorial plans till to constrained optimization.

2.4 References

- [1] Yu, L.; Koh, C. G.; Lee, L. J.; Koelling, K. W. Madou, M. J. (2002), Experimental investigation and numerical simulation of injection molding with micro-features. *Polymer Engineering & Science*, 42(5), 871-888;
- [2] Liu, C. Recent developments in polymer MEMS. (2007), *Advanced Materials*, 19.22: 3783-3790.
- [3] Wilson, K.; Molnar, P.; Hickman, J. (2007), Integration of functional myotubes with a Bio-MEMS device for non-invasive interrogation. *Lab on a Chip*, 7.7: 920-922.

- [4] Spatz, J. P. Building up micromuscles. (2005), *Nature materials*, 4.2, 115-116;
- [5] Pal, P.; Sato, K. (2009), Complex three-dimensional structures in Si {1 0 0} using wet bulk micromachining. *Journal of Micromechanics and Microengineering*, 19.10, 105008;
- [6] Heckeke, M.; Schomburg, W. K. (2003), Review on micro molding of thermoplastic polymers. *Journal of Micromechanics and Microengineering*, 14.3: R1.
- [7] Giboz, J.; Copponnex, T.; Mélé, P. (2007), Microinjection molding of thermoplastic polymers: a review. *Journal of micromechanics and microengineering*, 17.6: R96;
- [8] Tosello, G., Hansen, H. N. (2010), *Micro-Injection Molding. Micromanufacturing Engineering and Technology*. Amsterdam: Elsevier, 90-113.;
- [9] Tosello, G., Gava, A., Hansen, H. N., Lucchetta, G. (2010), Study of process parameters effect on the filling phase of micro-injection moulding using weld lines as flow markers. *The International Journal of Advanced Manufacturing Technology*, 47(1), 81-97.;
- [10] Griffiths, C. A., Dimov, S. S., Scholz, S., Hirshy, H., Tosello, G. (2011), Process factors influence on cavity pressure behavior in microinjection moulding. *Journal of manufacturing science and engineering*, 133(3).;
- [11] Surace, R.; Trotta, G.; Bellantone, V.; Fassi, I. (2012), The micro injection moulding process for polymeric components manufacturing, *New Technologies—Trends, Innovations and Research*, Chapter 4, INTECH Open Access Publisher;
- [12] Sha, B.; Dimov, S.; Griffiths, C.; Packianather, M. S. (2007), Micro-injection moulding: Factors affecting the achievable aspect ratios. *The International Journal of Advanced Manufacturing Technology*, 33(1), 147-156.
- [13] Shoemaker, J. (2006), *Moldflow design guide; a resource for plastic engineers*, Hanser Gardner Pub.
- [14] Zhang, H. L.; Ong, N. S.; Lam, Y. C. (2008), Mold surface roughness effects on cavity filling of polymer melt in micro injection molding. *The International Journal of Advanced Manufacturing Technology*, 37(11-12), 1105-1112.
- [15] Marson, S.; Attia, U. M.; Lucchetta, G.; Wilson, A.; Alcock, J. R.; Allen, D. M. (2011), Flatness optimization of micro-injection moulded parts: the case of a PMMA microfluidic component. *Journal of Micromechanics and Microengineering*, 21(11), 115024;
- [16] Dawson, A.; Rides, M.; Allen, C. R. G.; Urquhart, J. M. (2008), Polymer–mould interface heat transfer coefficient measurements for polymer processing. *Polymer Testing*, 27(5), 555-565;
- [17] Nakao, M.; Tsuchiya, K.; Sadamitsu, T.; Ichikohara, Y.; Ohba, T.; Ooi, T. (2008), Heat transfer in injection molding for reproduction of sub-micron-sized features. *The International Journal of Advanced Manufacturing Technology*, 38(3-4), 426-432;
- [18] Zhang, H. L.; Ong, N. S.; & Lam, Y. C. (2007), Effects of surface roughness on microinjection molding. *Polymer Engineering & Science*, 47(12), 2012-2019;
- [19] Zhang, H. L. (2008), *Numerical and Experimental Investigation on Cavity Roughness Effects in Micro Injection Molding* (Doctoral dissertation, PhD Thesis, School of Mechanical and Aerospace Engineering, NTU, Singapore).

- [20] Ong, N. S.; Zhang, H. L.; Lam, Y. C. (2009), Three-dimensional modeling of roughness effects on microthickness filling in injection mold cavity. *The International Journal of Advanced Manufacturing Technology*, 45(5-6), 481;
- [21] Nguyen, Q. M. P.; Chen, X.; Lam, Y. C.; Yue, C. Y. (2012), Effects of mold surface roughness on compressible flow of micro-injection molding. *World Acad. Sci. Eng. Technol.*, 65, 853-857;
- [22] Yao, D.; Kim, B. (2002), Simulation of the filling process in micro channels for polymeric materials. *Journal of micromechanics and microengineering*, 12(5), 604;
- [23] Cao, W.; Kong, L.; Li, Q.; Ying, J.; Shen, C. (2011), Model and simulation for melt flow in micro-injection molding based on the PTT model. *Modelling and Simulation in Materials Science and Engineering*, 19(8), 085003;
- [24] Yang, C.; Yin, X.-H.; Cheng, G.-M. (2013), Microinjection molding of microsystem components: new aspects in improving performance. *Journal of Micromechanics and Microengineering*, 23.9: 093001;
- [25] Jiang, B. Y.; Xie, L.; Tan, X. F.; Lu, S. Q. (2006), Influence of section shape of micro channels on microfluid flowability. *Journal of Central South University: Natural Science*, 37(5), 964-969;
- [26] Yang, C.; Huang, H. X.; Castro, J. M.; Yi, A. Y. (2011), Replication characterization in injection molding of microfeatures with high aspect ratio: Influence of layout and shape factor. *Polymer Engineering & Science*, 51(5), 959-968;
- [27] Attia, U. M.; Marson, S.; Alcock, J. R. (2009), Micro-injection moulding of polymer microfluidic devices. *Microfluidics and nanofluidics*, 7(1), 1;
- [28] Costa, F. S.; Tosello, G.; Whiteside, B. R. (2009), Best practice strategies for validation of micro moulding process simulation. *Polym. Process Engin*, 331-364;
- [29] Trotta, G.; Stampone, B.; Fassi, I.; Tricarico, L. (2021), Study of rheological behaviour of polymer melt in micro injection moulding with a miniaturized parallel plate rheometer. *Polymer Testing*, 96, 107068;
- [30] Lou, Y.; Bai, C.; Pei, J. L.; He, P. Q. (2016), A Novel Micro Wall Slip Model Based on Chain Length and Temperature. *International Polymer Processing*, 31(2), 239-246;
- [31] Rosenbaum, E. E.; Hatzikiriakos, S. G. (1997), Wall slip in the capillary flow of molten polymers subject to viscous heating. *AIChE journal*, 43(3), 598-608;
- [32] Lam, Y. C.; Wang, Z. Y.; Chen, X.; Joshi, S. C. (2007), Wall slip of concentrated suspension melts in capillary flows. *Powder Technology*, 177(3), 162-169;
- [33] Kim, D. S.; Lee, K. C.; Kwon, T. H.; Lee, S. S. (2002), Micro-channel filling flow considering surface tension effect. *Journal of Micromechanics and Microengineering*, 12(3), 236;
- [34] Nguyen-Chung, T.; Jüttner, G.; Löser, C.; Pham, T.; Gehde, M. (2010), Determination of the heat transfer coefficient from short-shots studies and precise simulation of microinjection molding. *Polymer Engineering & Science*, 50(1), 165-173;
- [35] Babenko, M.; Sweeney, J.; Petkov, P.; Lacan, F.; Bigot, S.; Whiteside, B. (2018), Evaluation of heat transfer at the cavity-

polymer interface in microinjection moulding based on experimental and simulation study. *Applied Thermal Engineering*, 130, 865-876;

[36] Dawson, A.; Rides, M.; Allen, C. R. G.; Urquhart, J. M. (2008), Polymer–mould interface heat transfer coefficient measurements for polymer processing. *Polymer Testing*, 27(5), 555-565;

[37] Nakao, M.; Tsuchiya, K.; Sadamitsu, T.; Ichikohara, Y.; Ohba, T.; Ooi, T. (2008), Heat transfer in injection molding for reproduction of sub-micron-sized features. *The International Journal of Advanced Manufacturing Technology*, 38(3-4), 426-432;

[38] Chen, C. S.; Chen, S. C.; Liaw, W. L.; Chien, R. D. (2008), Rheological behavior of POM polymer melt flowing through micro-channels. *European Polymer Journal*, 44(6), 1891-1898;

[39] Zhang, N.; Gilchrist, M. D. (2012), Characterization of thermo-rheological behavior of polymer melts during the micro injection moulding process. *Polymer testing*, 31(6), 748-758;

[40] Xie, L.; Niesel, T.; Leester-Schädel, M.; Ziegmann, G.; Büttgenbach, S. (2013), A novel approach to realize the local precise variotherm process in micro injection molding. *Microsystem technologies*, 19(7), 1017-1023;

[41] Xie, L.; Ziegmann, G. (2008), A visual mold with variotherm system for weld line study in micro injection molding. *Microsystem Technologies*, 14(6), 809-814;

[42] Su, Q.; Zhang, N.; Gilchrist, M. D. (2016), The use of variotherm systems for microinjection molding. *Journal of Applied Polymer Science*, 133(9);

[43] Zhang, N.; Zhang, H.; Stallard, C.; Fang, F.; Gilchrist, M. D. (2018), Replication integrity of micro features using variotherm and vacuum assisted microinjection moulding. *CIRP Journal of Manufacturing Science and Technology*, 23, 20-38;

[44] Yoon, S. H.; Padmanabha, P.; Cha, N. G.; Mead, J. L.; Barry, C. M. F. (2011), Evaluation of vacuum venting for micro-injection molding. *International Polymer Processing*, 26(4), 346-353;

[45] Sorgato, M.; Babenko, M.; Lucchetta, G.; Whiteside, B. (2017), Investigation of the influence of vacuum venting on mould surface temperature in micro injection moulding. *The International Journal of Advanced Manufacturing Technology*, 88(1-4), 547-555;

[46] Sorgato, M.; Masato, D.; Lucchetta, G. (2017), Effect of vacuum venting and mold wettability on the replication of micro-structured surfaces. *Microsystem Technologies*, 23(7), 2543-2552;

[47] Qiu, Z. J.; Zheng, H.; Fang, F. Z.; Wang, H. Y. (2012), Longitudinal ultrasound-assisted micro-injection moulding method. *Nanotechnol Precis Eng*, 10(2), 170-176;

[48] Michaeli, W.; Opfermann, D. (2006), Ultrasonic plasticising for micro injection moulding. In *4M 2006-Second International Conference on Multi-Material Micro Manufacture* (pp. 345-348). Elsevier;

[49] Michaeli, W.; Kamps, T.; Hopmann, C. (2011), Manufacturing of polymer micro parts by ultrasonic plasticization and direct injection. *Microsystem technologies*, 17(2), 243-249;

[50] Masato, D.; Sorgato, M.; Lucchetta, G. (2018), Effect of ultrasound vibration on the ejection friction in microinjection molding. *The International Journal of Advanced Manufacturing Technology*, 96(1), 345-358;

- [51] Tosello, G.; Gava, A.; Hansen, H. N.; & Lucchetta, G. (2010). Study of process parameters effect on the filling phase of micro-injection moulding using weld lines as flow markers. *The International Journal of Advanced Manufacturing Technology*, 47(1), 81-97.
- [52] Marhöfer, D. M.; Tosello, G.; Hansen, H. N.; Islam, A. (2013), Advancements on the simulation of the micro injection moulding process. In *Proceedings of the Multi-Material Micro Manufacture (4M) Int. Conf.*, San Sebastian, Spain (pp. 8-10);
- [53] Babenko, M.; Sweeney, J.; Petkov, P.; Lacan, F.; Bigot, S.; Whiteside, B. (2018), Evaluation of heat transfer at the cavity-polymer interface in microinjection moulding based on experimental and simulation study. *Applied Thermal Engineering*, 130, 865-876;
- [54] Chen, S. C.; Tsai, R. I.; Chien, R. D.; Lin, T. K. (2005), Preliminary study of polymer melt rheological behavior flowing through micro-channels. *International Communications in Heat and Mass Transfer*, 32(3-4), 501-510;
- [55] Ito, H.; Kazama, K.; Kikutani, T. (2007), Effects of Process Conditions on Surface Replication and Higher-Order Structure Formation in Micromolding. In *Macromolecular symposia* (Vol. 249, No. 1, pp. 628-634). Weinheim: WILEY-VCH Verlag;
- [56] Mnekbi, C.; Vincent, M.; Agassant, J. F. (2010), Polymer rheology at high shear rate for microinjection moulding. *International Journal of Material Forming*, 3(1), 539-542.
- [57] Vázquez, R. M.; Trotta, G.; Volpe, A.; Paturzo, M.; Modica, F.; Bianco, V.; Osellame, R. (2019), Plastic lab-on-chip for the optical manipulation of single cells. In *Factories of the Future* (pp. 339-363). Springer, Cham;
- [58] Trotta, G.; Volpe, A.; Ancona, A.; Fassi, I. (2018), Flexible micro manufacturing platform for the fabrication of PMMA microfluidic devices. *Journal of Manufacturing Processes*, 35, 107-117;
- [59] Haberstroh, E.; Brandt, M. (2002), Determination of mechanical properties of thermoplastics suitable for micro systems. *Macromolecular Materials and Engineering*, 287(12), 881-888.
- [60] Baruffi, F., Calaon, M., Tosello, G., (2018), Micro-Injection Moulding In-Line Quality Assurance Based on Product and Process Fingerprints. *Micromachines*, 9, 293;

Goal of the PhD activity

3.1 Part weight as the main observed variable

Micro injection moulding is a micro-fabrication technology which, more than any other, is proposed as a technology for mass production of micro components. For the definition already given by Sha et al [1], now widely shared by the scientific world, we can identify two types of micro components, namely plastic components on which are reproduced microfeatures and micrometric components in the order of a few milligrams.

Although the micro-moulding process was considered as a scale factor of the traditional injection moulding at an early stage of technological development, the great differences between the two processes were gradually recognised, differences mainly related to the fast cooling of the micro cavity, due to the reduced size of the cavity compared to the entire master mould, and the different viscous behaviour of the material in the micro cavities. This last aspect, in particular, is related to the high aspect ratio of the cavity so that physical properties that in standard injection moulding are generally negligible, as for example roughness, becomes proportional to the thickness, and brings about thermal diffusivity and wall-slip phenomena that alter the polymer apparent fluid-phase viscosity [2, 3].

The process differences described led to the creation of machines specifically dedicated to micro injection moulding. These are machines capable of reaching speeds of an order of magnitude higher than the standard ones, and therefore able to transfer the material much faster in cavities, this in order to compensate the high cooling rate and prevent premature solidification of the material at the gate and resulting in incomplete filling of the cavity.

The increase in process speeds, however, introduced two rather important requirements, namely on the one hand, much precise and reliable control of metering size, and on the other hand the need for higher injection pressures. These two aspects push micro injection moulding machines to an advanced technology level than standard ones, leaving almost completely the hydraulic system to exclusively marry the "full electric" in order to have a better control of the dynamics and consequently improve in precision and reliability.

What has been highlighted is that micro injection moulding is an emerging new technology which prospects still need to be fully discovered with related problems of process reliability.

Several studies have focused on the analysis of the reliability of the micro injection moulding process, and in particular on aspects characterizing the process itself, such as the filling phase, the analysis of shrinkage, the cavity pressure distribution, the component weight. Through the study of the process parameters and the observation of the defects, some problems of micro injection moulding could be highlighted.

The use of high dynamics results in a high variability of the injected charge, a problem mainly related to the reactivity of the numerical control while going from high acceleration phase to high deceleration phase (filling phase) that results in a less precise position control at the switchover point, where the machine switch from volumetric control to pressure control. This results in a large variability of the filling conditions, which can affect the following packing (or holding) phase, with consequent overpacking effect, when the material injected in the cavity is excessive, or short shots effect, when the material is lower than expected. In the case of overpacking, in particular, one of the main consequences is the difficulty of extraction, with the risk of damaging the component.

Analysis of pressure distribution in cavities has shown that rather high injection pressures are needed to contrast the excessive pressure drop that is detected in cavities due to the high aspect ratio [4]. However, in some cases, the combination of the parameters necessary for the complete filling of the cavity leads to exceed the machine clamping force limit for a short time resulting in the production of flash, a rather widespread defect in micro injection moulding that is difficult to reduce due to the small process window. There is a clear difficulty in defining methods to analyse the quality of the micro component for the small size of the components themselves, as well as for the high process speed. Cavity pressure monitoring is very complex to perform because even if the size of the sensors is small, they require an housing space that is often not available and monitoring must be accepted in areas that are not particularly significant compared to the most appropriate ones. At the same time, optical systems for the rapid identification of faults or in any case for the measurement of parts of the moulded microcomponent are not available and quite often the measurements are made with optical systems "off line".

From this analysis clearly emerges that the part weight could be, for the micro injection moulding, the element of synthesis for a rapid feedback on the quality and reliability of the process. Measuring the weight of the micro component, in fact, is conceptually very easy to achieve "in line" at the end of each cycle and would allow operators to automatically monitor the process with the implementation of the closed loop.

3.1.1 State of the art of part weight

Few articles have focused their research on the analysis of the part weight in the micro injection moulding process. The approach typically used is an experimental plan based on Design of

Experiments, mainly factorial plans, to make a preliminary screening of the process and to find a model that correlates the process parameters with the observed variable “part weight”. Then optimization approach based mainly on desirability function has been used to identify the feasible part weight and the related range of the statistically significant factors.

Attia et al [5], in a first paper presented in 2009, for the first time introduced the part weight as an output parameter to reflect the filling of five separate parts with different micro-feature designs moulded with Polymethylmethacrylate (PMMA). Five processing parameters, namely mould temperature, melt temperature, injection speed, hold pressure and cooling time, are investigated using a screening half-factorial experimentation plan, with Resolution-V, to determine their possible effect on the filling quality of the moulded parts. After preliminary process stabilisation through a short moulding phase, ten samples were randomly collected for each run. The average weight of the samples was recorded as the experiment response. From the analysis of the results it emerges a significant effect of holding pressure for all the five parts. The importance of holding pressure lies in the fact that it overcomes the tendency of the polymer melt to prematurely freeze before the injection process is complete. Premature freezing is related to the high rate of heat transfer between the polymer and the mould walls for parts with micro-scaled dimensions. For the authors, instead, the lack of significance of cooling time [6, 7] is related to the fact that the effect of cooling in injection moulding is usually associated with changes in the component geometry (e.g. shrinkage, warpage) [8], but the cooling scheme does not have the same effect on the part weight as its effect takes place after the cavity is already filled. The lack of significance of mould temperature, instead, may lie in the selection of the two levels at values below the glass transition temperature (T_g) of the polymer while increasing the mould temperature can significantly improve the filling quality [9]. The lack of significance of melt temperature is probably related to the polymer contact with the cavity walls that are at the mould temperature below the T_g [10]. Hence, by the time the polymer filled the part cavity it would have seen a significant reduction in its temperature. Finally, the lack of significance of the injection velocity as a parameter may lie in the relatively small change of shear rate associated with changing between the two levels of injection velocity [8]. After the screening stage, the optimization was carried out using the desirability function approach to calculate optimum values of the input parameters. The desired part weights were derived from the screening experiments. The moulded samples are inspected, and the completely filled samples are identified and weighed. The average weight of complete samples is used as the “target” weight for the desirability function. The minimum and maximum weights of the completely filled samples are input as the lower and upper limits for the target weight, respectively. A comparison of desirable moulding parameters for different part geometries, showed the influence of geometry on processing conditions.

The methodology implemented in [5] has been used also in their other papers [11] and [12], but this time focalizing on complex geometries and different materials. They tried to identify the

influence of other parameters on the part weight and to improve knowledge analysing also the weight variation in terms of standard deviation of the replicated part weight. It was found that holding pressure, melt temperature and injection velocity were statistically significant for part weight, whereas injection velocity alone was significant for weight variation.

This methodology has been replicated by Bellantone et al. [13] on a “dog bone” test specimen moulded with the most suitable materials for micro injection moulding due to their flowability: pure POM and LCP (glass reinforced). The purpose is to investigate the effect of micro injection process parameters on part weight and on its standard deviation, and overall dimensions of a moulded miniaturised tensile test specimen. The process parameters considered for the experimentations are mould temperature, melt temperature, injection speed and holding pressure and time. It has been found that the holding pressure and holding time for POM and holding pressure and injection velocity for LCP have the highest influence on achieving high part weight. Differently, melt temperature has the highest influence on minimising the process variability for both tested polymers. A further investigation has been carried out on the relationship between the holding pressure and the part weight and dimensions demonstrating the existence of a linear correlation between specimen weight and dimensions.

In [14], the authors tried to implement a statistical methodology to optimise both shrinkage and part weight in micro-injection moulding. Five factors were investigated: the injection pressure, the holding pressure, the melt temperature, the mould temperature and the holding time. The mould and melt temperatures and the holding pressure were identified as significant factors that affect both shrinkage in parallel to the flow direction and part weight independently. In addition, shrinkage in parallel to the flow direction is affected by combined effect of holding pressure-mould temperature and melt temperature-mould temperature. Optimal conditions for the minimisation of the total shrinkage and maximisation of part weight were determined using desirability functions.

Eladl et al. [15] studied the effect of four process parameters (melt temperature, mould temperature, holding pressure and injection velocity) on the quality characteristics of polymeric parts produced by micro injection moulding observing part mass, flow length and flash formation according to a Design of Experiment approach. Holding pressure and injection speed were found to be the most effective on mass and flow length for both the used materials and micro cantilever geometries with variable thickness. Injection speed and packing pressure have direct effect on the flow length, increasing it inversely proportional to the thickness of the cantilever geometries. Injection speed and holding pressure had higher effects than melt and mould temperature and were the most affective parameters on increasing the amount of flash for both materials when set at high levels.

A literature review comparison is shown in Table 3.1. It clearly emerges how it is difficult to generalize the results of the literature because of the different μ IM systems, samples and material used. However, it appears that holding pressure, melting temperature and

injection speed are the most significant factors affecting the part weight.

3.2 Constraints related to the part weight

Typical defects that occur while processing micro injection moulding are the same observed for the standard process. They can be classified in internal defects, which usually are shrinkage, weld lines, flow lines and jetting; surface defects, such as sink marks, gas burns (diesel effect) and ejection marks; geometrical defects, that usually are incomplete filling (short shot), flash and warping.

These defects directly affect the principal characteristics typically evaluated to certify the final quality of the polymeric part: mechanical properties, part weight, form and dimensions, surface aspect. So, their correct detection is essential to prevent the non-conformities of the products.

Most of these defects are identified, in the case of the standard process, by visual checks during production, such as the case of burns, sink marks, filling defects, ejection marks, geometric defects. Only in some cases it is implemented a destructive approach on a statistical basis or with density measurements, especially for internal defects.

In the case of micro injection moulding, the dimensions involved do not allow a clear visual identification of most of these defects, which are often at micrometric level. Any type of inspection, whether visual or destructive, requires a microscope inspection for clear evidence and this complicates the evaluation of the quality of the process and extend the time to eventually correct the process, resulting in large amounts of waste.

In literature, the study of the micro injection moulding process often focuses on the analysis of process parameters that most affect the quality of the product by directly observing some of the defects described and implementing an optimization approach of the defects themselves, in terms of minimization, or optimizing a characteristic such as weight or geometric shape, indirectly obtaining an assessment of the effectiveness of the proposed approach in order to minimize the defects themselves.

Several authors used a Design of Experiment approach to identify the process parameters that mainly affect the observed variable and consequently to identify a subset of parameters on the basis of which to implement an optimization method based on Taguchi approach, as reported below. Other authors, as seen in the previous section for the part weight variable, used the optimization approach based on desirability function [1,7--10].

Erzurumlu et al. [16] and Chang et al [17] implemented an orthogonal array of Taguchi, the signal-to-noise (S/N) ratio, and analysis of variance (ANOVA) to find the optimal levels and the effect of process parameters on warpage and sink index [16] and on formability of microstructure and mechanical properties [17]. Both optimization approaches are based on a full factorial, three level, design. In order to reduce the time and experimental cost, a reduced number of the trials were used to implement the L18 orthogonal array. For [16] Packing pressure is the most influencing factor for PC, ABS and POM while melt temperature more than mould

temperature and packing pressure for PA66. For [17] mould temperature and injection speed are the most important process parameters.

The research proposed by [18] investigates the effects that the tool coating can have on part demoulding in micro injection moulding. One method that can be used for improving the wear resistance of tool surfaces is to apply surface treatments. Taguchi L9 orthogonal array (OA) was employed (four factors at three levels) to ensure that the experimental results were representative of the considered processing window. Based on the experimental results, an analysis of variance (ANOVA) was performed in order to assess the contribution of each processing parameter to the resulting demoulding behaviour.

Shen et al [19] implemented a general experimental approach to achieve a rapid cavity filled stage and reduce shrinkage. The optimal parameters for the thin-wall microinjection moulding are found, namely the injection speed, injection pressure and mould temperature, which can achieve a rapid cavity filled stage and reduce shrinkage effects.

In Chien et al [20], a set of systematic experiments was conducted to examine the effects of process parameters on the replication accuracy of microchannels. They found that the accuracies of the imprint width and depth increased with increasing mold temperature, melt temperature, injection velocity and packing pressure within regular processing window.

Annichiarico et al. [21] provide a method for measuring shrinkage in micro injection moulded (m-IM) parts. Clear differences in shrinkage between parallel and normal to the flow direction were found. Furthermore, differences between moulding, post-moulding and total shrinkage were observed. Mould temperature affected moulding shrinkage both parallel and normal to the flow but the direction of the effect was different. For post-moulding shrinkage, only shrinkage normal to the flow was affected by factors investigated in this study: a combination of holding time and mould temperature. However, for total shrinkage, only the shrinkage parallel to the moulding direction was affected by three factors and two combinations of factors. No statistically significant effects were observed for total shrinkage normal to the flow, and post-mould shrinkage parallel to the flow.

Baruffi et al. [22] proposed a methodology to predict flash formation at micro level. The approach was based on a set-up of simulation model so that small extensions of the model in areas where, previously by experimental trials, it was observed flash. The simulation was compared with experimental DoE plan using a focus variation microscope and the results are an overestimate of flash for the model compared to the experimental trials while the process parameters were well predicted by the numerical model.

In Table 3.2 is reported a review comparison related to the different approaches used to identify and minimize some of the typical defects of micro injection moulding process.

What emerges from this analysis of the state of the art regarding the micro injection moulding is that this process has been extensively investigated from the scientific point of view in the last fifteen years. The researchers are still evaluating the influence of the process

parameters on process characteristics and defects, identifying possible models and defining guidelines for near-zero defect part micro manufacturing. Most of the work analysed treat the defects and their containment indirectly by observing, for example, the general quality of the component or through microscopic observations or by measuring process parameters in cavities. Only some cases report about possible interaction between two variables, one related to the process characteristics, such as part weight, and the other to some defects, such as shrinkage effect [14] or flash [15]. According to the analysis reported, the idea is that the micro injection moulding can be considered a process ready for the industrial world, and in fact the micro injection molding machine market size is estimated to growth of 9.8% between 2021 and 2026 [23]. Medical filed is estimated to be the largest application of the micro injection moulding market in the next years, and this is in agreement with the large scientific interest in biomedical and microfluidic geometries, as seen in the previous chapter. However, despite these strong process developments, a level of automation and quality control comparable to that achieved by standard injection molding is still far away and requires further research.

While some significant progress has been achieved in building models for inline and real-time process control [24-26], the complexity of implementing cavity sensors for process control in a mould for micro, or an online vision system for quality control, limit the full industrial development of the process that is still very linked to the sensitivity of the operator and the experience made in the field rather than to the implementation of methodologies and procedures developed by the scientific world. It seems necessary to further contribute to the process development and in particular to the technology transfer from the scientific world to the industrial world, focusing more on concrete industrial applications, to have a closer response to the real production needs, and developing optimization procedures whose inputs are values related to variables easily manageable and measurable by machine tool operators.

3.3 Description of the original idea

The purpose of the PhD project is to identify a response variable that allows to monitor the process and easy to measure at the same time. The purpose it to make it easy to implement, this procedure in any company interested in micro injection moulding technology providing a tool for which operators feel confident to use it and that can help to solve one of the most challenging aspects of micro injection moulding manufacturing, the lack of reliability in terms of ability to replicate the process.

Even if starting from a common approach to what emerged from the state of the art, so from a Design of Experiment approach based on a factorial plan, the idea is to go beyond the analysis of variance to identify the most influential process parameters and subsequent optimization based on the largely used criterion of desirability that requires additional experimental cost.

The idea behind the PhD work is to observe, with an experimental approach, both the weight variable, which is a continuous variable, and the related flash defect, which is instead a categorical variable because it is defined on a basis of subsequent evaluations to observation. This approach is very useful because it follows, and somehow combines, the industrial methodology, which always prefers a direct observation of part to classify the quality and eventually the defect due to personal sensitivity and experience, with the scientific world that instead, with a statistical approach, seeks to identify reliable models for assessing the quality of the product.

The in-depth analysis of the state of the art on the weight variable clearly showed how much this variable is of scientific interest, but above all also for industrial, for its ease of measurement and at the same time complexity in the evaluation of the result, in the sense that it is not always correct to identify as weight maximization the objective function that you want to achieve. The presence of flash, a rather frequent defect in micro injection moulding, is one of the defects that can most alter this objective. In addition, its identification and cataloguing is subject to the sensitivity and experience of the operator and this can be an additional disturbing element in the correct evaluation of the maximum weight.

This evaluation, in fact, gives rise to the most ambitious objective of the doctoral work, that is to identify a model that considers at the same time the maximization of weight in a region where the absence of flash can be expected with good probability.

Although simple in describing it, however it is not so simple because while the weight variable is quantitative, the flash variable is categorical and closely related to the weight variable. Therefore, the main objective of this work is to identify a region of eligibility of the optimal weight constrained by the probability of having flash.

3.4 References

- [1] Sha, B.; Dimov, S.; Griffiths, C.; Packianather, M. S. (2007), Investigation of micro-injection moulding: Factors affecting the replication quality. *Journal of Materials Processing Technology*, 183(2-3), 284-296.
- [2] Zhang, N.; Gilchrist, M. D. (2012), Characterization of thermo-rheological behavior of polymer melts during the micro injection moulding process, *Polymer testing*, 31(6), 748-758.
- [3] Trotta, G.; Stampone, B.; Fassi, I.; Tricarico, L. (2021), Study of rheological behaviour of polymer melt in micro injection moulding with a miniaturized parallel plate rheometer, *Polymer Testing*, 96, 107068;
- [4] Mendibil, X.; Llanos, I.; Urreta, H.; Quintana, I. (2017), In process quality control on micro-injection moulding: The role of sensor location. *The International Journal of Advanced Manufacturing Technology*, 89(9-12), 3429-3438.
- [5] Attia, U. M.; Alcock, J. R. (2009), An evaluation of process-parameter and part-geometry effects on the quality of filling in micro-injection moulding, *Microsystem technologies*, 15.12: 1861;

- [6] Zhao, J.; Mayes, R.; Chen, G.; Xie, H.; Chan, P. (2003), Effects of process parameters on the micro molding process. *Polym Eng Sci*, 43:1542–1554;
- [7] Zhao, J.; Mayes, R.; Chen, G.; Chan, P.S.; Xiong, Z.J. (2003), Polymer, micromould design and micromoulding process. *Plast Rubber Compos*, 32:240–247;
- [8] Osswald, T.; Turng, L.; Gramann, P. (2001), Injection molding handbook. Hanser/Gardner Publications, Cincinnati;
- [9] Shen, Y.K.; Yeh, S.L.; Chen, S.H. (2002), Three-dimensional non-Newtonian computations of micro-injection molding with the finite element method. *Int Commun Heat Mass*, 29:643–652;
- [10] Yao, D.; Kim, B. (2004), Scaling issues in miniaturization of injection molded parts, *J Manuf Sci Eng Trans ASME*, 126(4):733–739;
- [11] Attia, U. M.; Alcock, J. R. (2010), Optimising process conditions for multiple quality criteria in micro-injection moulding, *The International Journal of Advanced Manufacturing Technology*, 50.5: 533-542;
- [12] Attia, U. M.; Alcock, J. R. (2011), Evaluating and controlling process variability in micro-injection moulding, *The international journal of advanced manufacturing technology*, 52.1: 183-194;
- [13] Bellantone, V.; Surace R.; Trotta G.; Fassi I., (2013), Replication capability of micro injection moulding process for polymeric parts manufacturing. *The international journal of advanced manufacturing technology*, 67.5-8: 1407-1421;
- [14] Annicchiarico, D.; Attia, U. M.; Alcock, J. R. (2013), Part mass and shrinkage in micro injection moulding: Statistical based optimisation using multiple quality criteria, *Polymer Testing*, 32.6: 1079-1087;
- [15] Eladl, A.; Mostafa, R.; Islam, A.; Loaldi, D.; Soltan, H.; Hansen, H.N.; Tosello, G. (2018), Effect of Process Parameters on Flow Length and Flash Formation in Injection Moulding of High Aspect Ratio Polymeric Micro Features, *Micromachines*, 9, 58.
- [16] Erzurumlu, T.; Ozcelik, B. (2006), Minimization of warpage and sink index in injection-molded thermoplastic parts using Taguchi optimization method. *Materials & design*, 27(10), 853-861;
- [17] Chang, P. C.; Hwang, S. J. (2006), Injection molding of microprobe array parts. *Journal of Polymer Research*, 13(1), 25-32.
- [18] Griffiths, C. A.; Dimov, S.; Brousseau, E. B.; Chouquet, C.; Gavillet, J.; Bigot, S. (2008), Micro-injection moulding: surface treatment effects on part demoulding, *Proc 4M2008 (Cardiff, UK, 9th–11th September 2008)*.
- [19] Shen, S. C.; Pan, C. T.; Wang, Y. R.; Chang, C. C. (2006), Fabrication of integrated nozzle plates for inkjet print head using microinjection process. *Sensors and Actuators A: Physical*, 127(2), 241-247;
- [20] Chien, R. D. (2006), Micromolding of biochip devices designed with microchannels. *Sensors and actuators A: physical*, 128(2), 238-247.
- [21] Annicchiarico, D.; Attia, U. M.; Alcock, J. R. (2013), A methodology for shrinkage measurement in micro-injection moulding, *Polymer testing*, 32(4), 769-777.
- [22] Baruffi, F.; Calaon, M.; Tosello, G. (2018), Prediction of micro-sized flash using micro-injection moulding process simulations. In

Proceedings of the 18th International Conference & Exhibition of the European Society for Precision Engineering and Nanotechnology (euspen), (pp. 263-264).

[23] <https://www.marketsandmarkets.com/Market-Reports/micro-injection-molding-machine-market-245710637.html>;

[24] Modoni, G. E., Stampone, B., Trotta, G. (2022), Application of the Digital Twin for in process monitoring of the micro injection moulding process quality, *Computers in Industry*, 135, 103568;

[25] Baruffi, F., Calaon, M., Tosello, G., (2018), Micro-Injection Moulding In-Line Quality Assurance Based on Product and Process Fingerprints. *Micromachines*, 9, 293;

[26] Baruffi, F., Gülçür, M., Calaon, M., Romano, J. M., Penchev, P., Dimov, S., Whiteside, B, Tosello, G. (2019), Correlating nano-scale surface replication accuracy and cavity temperature in micro-injection moulding using in-line process control and high-speed thermal imaging. *Journal of Manufacturing Processes*, 47, 367-381.

Table 3.1: Comparison of the literature on part weight optimization in μIM (X means that the factor was varied in the experiment, * indicates the significant factors in the analysis).

Paper	Material	Response	Mould temperature	Melt temperature	Injection speed	Holding pressure	Cooling time	Holding time	Injection Pressure	Result
[5]	PMMA	Part weight	X *	X	X *	X *	X			Holding pressure, injection speed and mould temperature are significant factors to control part geometries and part weight. Significant effect of holding pressure for all the five parts tested.
[11]	PMMA	Part weight	X	X *	X *	X *	X			Holding pressure, melt temperature and injection speed are significant for part weight and can be optimised within the initially specified upper and lower levels.
[12]	PMMA	Part weight Variability	X	X * *	X *	X *	X			Holding pressure, melt temperature and injection velocity were statistically significant for part weight, whereas melt temperature alone was significant for weight variation for one of the two produced parts.
[13]	POM LCP	Part weight Variability	X	X * * *	X *	X * *		X *		Holding pressure, holding time and melt temperature are significant for POM part weight. Holding pressure, injection speed and melt temperature are significant for LCP.
[14]	POM	Part weight	X *	X *		X *		X	X	Mould temperature, melt temperature, holding pressure, and their interactions, affect both shrinkage and part weight. The optimized values are the results of a compromise between shrinkage minimization and part weight maximization.
[15]	ABS PP	Part weigh Flow length Flash	X	X	X * * *	X * * *				Holding pressure and injection speed were the most effective on mass and flow length for both materials. Injection speed and holding pressure had higher effects than melt and mould temperature and revealed to be the most affective parameters on increasing the amount of flash for both material when set at high levels.

Table 3.2: Comparison of the literature on Taguchi and ANOVA optimization approach for minimizing most common defects in μ IM (X means that the factor was varied in the experiment, * indicates the significance levels of factors in the analysis ($\alpha= 0.05$)).

Paper	Material	Response	Mould temp.	Melt temp.	Injection speed	Holding pressure	Cooling time	Holding time	Injection Pressure	Switchover position	Delay before ejection	Clamping force	Cycle time	Result
[16]	PC/ABS POM PA66	Warpage Sink index	X *	X *		X *								For PC/ABS and POM the holding pressure is the most influential factor for both responses, while mould and melt temperature for PA66 in addition to packing pressure.
[17]	(PC) PP	Part geometry	X *	X *	X *	X	X	X	X	X				Injection speed and mold temperature are the most important factors affecting the quality of the microprobes.
[18]	PC ABS	Coated (*uncoated Demoulding tool	X * (*) * (*)	X (*) * (*)			X *				X * (*)			Mould temperature is the factors that more than any other affect the demoulding for both parameters. Improvements in the demoulding performance for coated tool.
[19]	LCP	High cavity filling, shrinkage	X *	X	X *				X *			X	X	A high injection speed, pressure and mold temperature can achieve a rapid cavity filled stage and reduce shrinkages
[20]	PMMA	replication accuracy	X *	X *	X *	X *								Higher mold temperature, melt temperature, injection velocity and packing pressure can lead to better replication accuracy for vacuum situation
[21]	POM	shrinkage	X *	X *		X *		X	X					Mould temperature is the most influencing factor for shrinkage together with holding pressure and melt temperature.
[22]	POM	flash	X *	X	X *	X *								Holding pressure is the most influencing factor for flash formation, together with mould temperature and injection speed.

Methodologies and tools to build the weight and flash datasets

4.1 Part weight as the main observed variable

According to the analysis of the previous chapter, the part weight has been identified as the affordable variable to predict the quality of the final part and some defects, such as flash, has been evaluated in order to identify the optimal region of part weight.

The material used for experiments is POM (polyoxymethylene), a polymer largely used in micro injection moulding due to its flowability that foster the filling of very small cavities.

In Table 4.1 the mechanical and physical properties of POM are reported. POM finds application in micro gears and micro filters for medical industries.

Table 4.1: POM main properties¹

Properties	Unit	Values
Density	kg/m ³	1400
Tensile modulus	MPa	2700
Yield stress, 50 mm/min	MPa	65
Yield strain, 50 mm/min	%	9.4
Coefficient of linear thermal expansion, longitudinal (23-55)°C	10 ⁻⁶ /K	110
Molding shrinkage (parallel)	%	2.10
Molding shrinkage (normal)	%	2.10

The machine used for experimentation is the DESMA Tec Formica Plast 1K which can inject up to 150 mm³ with a maximum speed of 500 mm/s at 3000 bar and with a clamping force of 10kN, Figure 4.1 **Errore. L'origine riferimento non è stata trovata.**a.

The part identified for the experimentation is a benchmark for micro injection moulding, a double thin plate component with thickness of 500 μm, a nominal part weight (POM) of 95,8 mg and an aspect ratio of about 8. The aspect ratio is defined as the ratio between the larger side (3.9 mm) and the smaller side (0.5 mm) of the rectangular section, see Figure 4.1b.

¹ https://plastics-rubber.basf.com/global/en/performance_polymers/products/ultraform.html

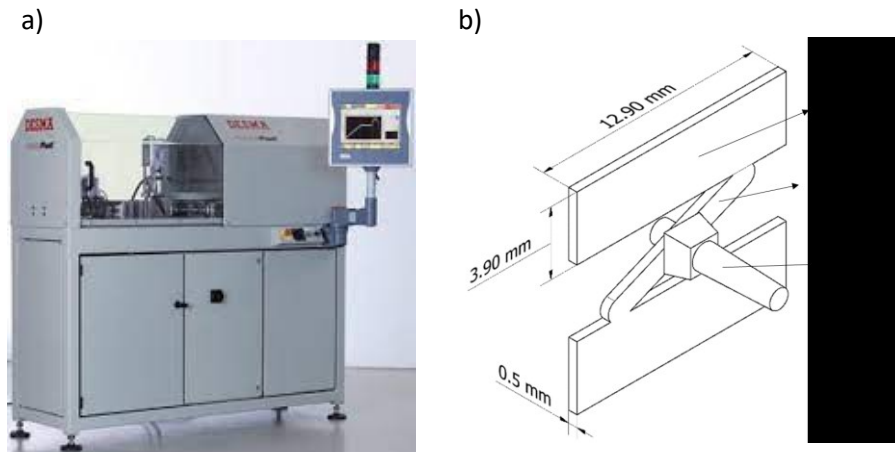


Figure 4.1: a) DESMA Tec Formica Plast 1K and b) details of the micro moulds and injected part with general dimensions

The mould has been designed considering n.5 ejectors in specific positions: at the beginning and at the end of the thin plate, and right under the sprue. The holes, that face the cavity, have been realized with a tolerance to ensure air evacuation while polymer fill the cavity, but preventing polymer outflow trough them. The lack of burn marks on the moulded parts produced in this work proves the correctness of the proposed solution.

Preliminary check on the reliability of the measuring system of the part weight has been carried out in section 4.1. Then the evaluation of the sigma of the machine has been investigated in section 4.2 in order to define the minimum number of replicas through the power analysis. Finally, the experimental plan adopted and the methodology to define the flash defect has been reported in section 4.3 while in section 4.4 are presented the criteria used to define the datasets for the identification of flash and weight models.

4.2 Check of the measurement tool error

In order to check the quality of the data obtained, a survey was carried out to verify the calibration of the balance. Certified weights were used and the weighing was carried out by two operators with different attitudes in random order. A 2-factor plan (weigh and operator) was prepared and the calibration points were 1 g, 2 g, 3 g, 4 g, 5 g with 2 replicates. Below is an image of the setup used which also included a temperature control in the weighing area (Fig. 4.2).



Fig. 4.2: overview of the set up to check the accuracy of the balance calibration

Table 4.2: Analysis of variance for the balance calibration check

Factor Information

Factor	Type	Levels	Values
Random operator	Fixed	2	1; 2
random weights	Fixed	5	1; 2; 3; 4; 5

Analysis of Variance

Source	DF	Adj SS	Adj MS	F-Value	P-Value
Operator random	1	0,000	0,0000	1,69	0,201
random weights	4	97,999	24,4997	2,43735E+09	0,000
random operator * random weights	4	0,000	0,0000	0,51	0,726
Error	40	0,000	0,0000		
Total	49	100,002			

Model Summary

S	R-sq	R-sq(adj)	R-sq(pred)
0,0001003	100,00%	100,00%	100,00%

The analysis of variance reported in Table 4.2 evidenced, in the Model Summary, that the resolution of 0,1 mg reported in the datasheet of the Gibertini Balance is correct.

As we can see from the Main effect plot of figure 4.3a, the operator hasn't effect on the measure that is influenced, as expected, by the calibration weights. The residuals are normally distributed (Fig. 4.3b), there are no outliers and all the data are in the interval [+3; -3] (Fig. 4.3c). The Bartlett test for normal distribution evidenced that the equal variance can't be rejected (Fig. 4.3d)

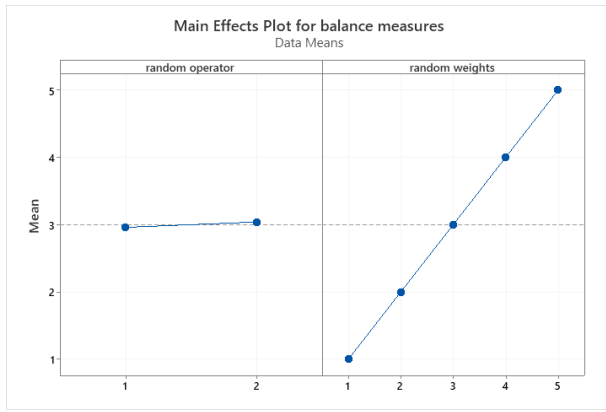


Fig. 4.3a: Main effect plot

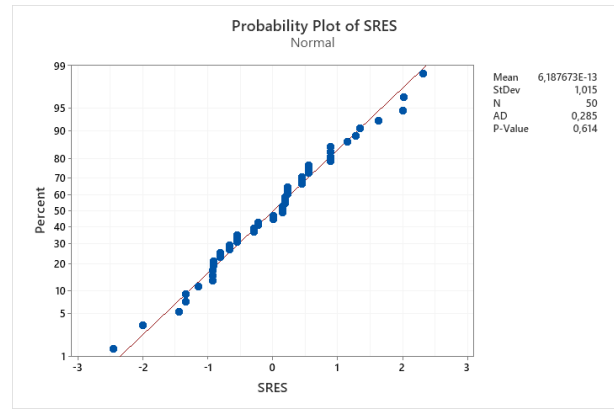


Fig. 4.3b: Probability plot of Standardized residuals

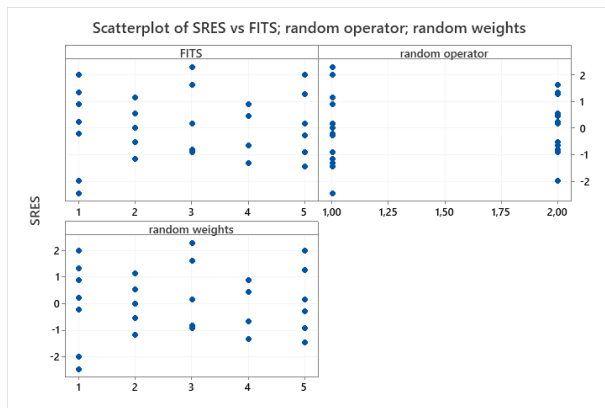


Fig. 4.3c: Scatterplot for outliers evaluation

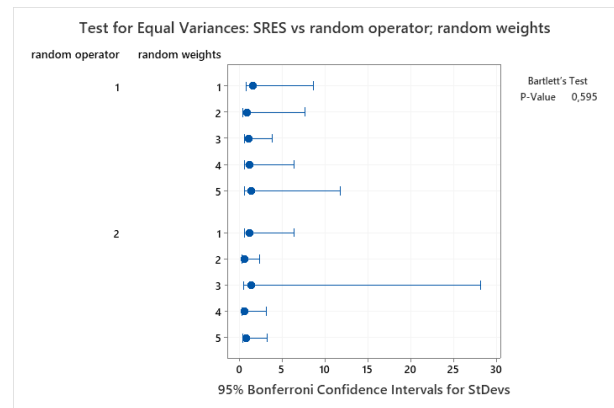


Fig. 4.3d: Test for equal variance hypothesis

4.3 Power analysis and evaluation of the sigma of the process

In order to determine the number of replicates used in the study of the micro injection moulding process, it was necessary to carry out a preliminary trial for the determination of sigma (σ) of the process. In the Table 4.3 it is reported the center point of the process parameters identified for the experimentation:

Tab.4.3: Center point process parameters

TRIAL	Tmold	Tmelt	Vinj	Phold	thold
	°C	°C	mm/sec	bar	sec
17	80	210	125	1000	2

Where Tmold is mould temperature, Tmelt is the melt temperature, vinj is the injection speed, Phold is the packing (holding) pressure and thold is the packing (holding) time.

In order to obtain a correct evaluation of the sigma of the process to be used for the Power Analysis, the experimental part has been printed n. 11 times, of which only the last printed one has been used for the measurement of the weight. This operation has been repeated for 6 times at a distance of about an hour from each other,

turning the machine off, cooling down the mould temperature, turning on the machine and heating up the mould again. In the following Tab 4.4 the sequences of measurement (mean and standard deviation) are reported consisting of n. 3 weight measurements carried out in sequence for each repetition, each one performed by switching off and after a few minutes on the precision balance and recalibrating it (Gibertini E154 with max weight 150 g, resolution 0,1 mg and error di 1 mg).

Tab.4.4: Weight measurement in the center point

WEIGHT MEASUREMENT IN THE CENTER POINT						
TRIALS	MEASUREMENT [g]			MEASUREMENT [mg]		
	1	2	3	1	2	3
1	0,0872	0,0873	0,0870	87,2	87,3	87,0
2	0,0916	0,0914	0,0915	91,6	91,4	91,5
3	0,0911	0,0912	0,0910	91,1	91,2	91,0
4	0,0903	0,0900	0,0901	90,3	90,0	90,1
5	0,0880	0,0881	0,0882	88,0	88,1	88,2
6	0,0911	0,0912	0,0912	91,1	91,2	91,2
					mean	89,86
					std. Dev.	1,70

In Fig. 4.4 we plot the data of center point analysis done and we can see that the three measurements for each trial are very close (balance precision).

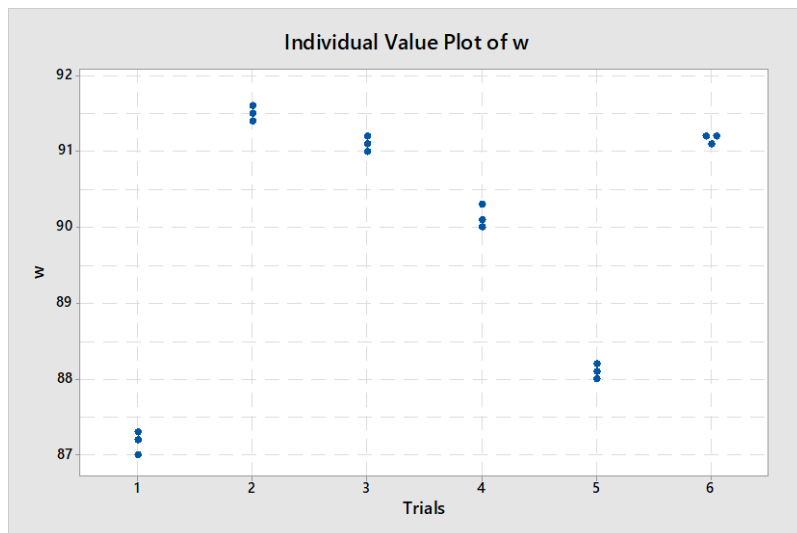


Fig. 4.4: Individual value plot for weight of the measurements of Tab. 4.2

The power of a hypothesis test is the probability that the test correctly rejects the null hypothesis. The power of a hypothesis test is affected by the sample size, the difference, the variability of the data, and the significance level of the test. If a test has low power, you might fail to detect an effect and mistakenly conclude that it does not exist. If a test has power that is too high, very small and possibly uninteresting effects might seem to be significant.

According to the results, we set on Minitab© all the parameters necessary to implement the Power Analysis test, useful to identify the minimum number of replicates necessary to detect an effect that might be significant.

In the following Fig. 4.5 are reported the details of the Power Analysis settings and the results obtained.

Power and Sample Size

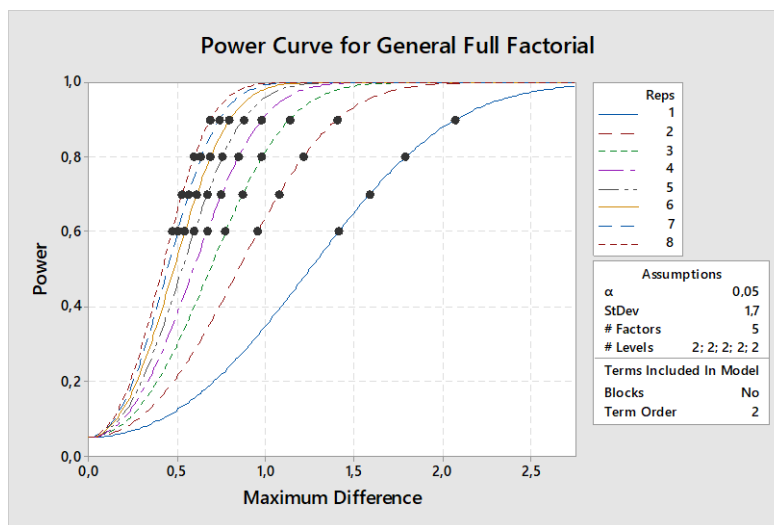
General Full Factorial Design

$\alpha = 0,05$ Assumed standard deviation = 1,7

Factors: 5 Number of levels: 2; 2; 2; 2; 2

Include terms in the model up through order: 2

Not including blocks in model.



Total Reps	Runs	Power	Maximum Difference
1	32	0,9	2,07670
1	32	0,8	1,79383
1	32	0,7	1,59006
1	32	0,6	1,41606
2	64	0,9	1,40607
2	64	0,8	1,21517
2	64	0,7	1,07752
2	64	0,6	0,95991
3	96	0,9	1,13860
3	96	0,8	0,98405
3	96	0,7	0,87261
3	96	0,6	0,77738
4	128	0,9	0,98260
4	128	0,8	0,84924
4	128	0,7	0,75307
4	128	0,6	0,67089
5	160	0,9	0,87717
5	160	0,8	0,75812

Fig. 4.5: Power curves of replicas for maximum difference

Remarks:

- The injection plunger has a diameter of 3 mm and for 1mm run, with polymer POM density of 1,4 g/cm³, in the machine inlet in the cavity 9,8 mg of material;
- The machine control has a response time of about 1 ms and this means that in 1 ms, at 100 mm/s, the machine injects in the cavity about 1 mg;
- The balance has an average error of 1 mg with resolution of 0,1 mg;

Considering previous remarks, we can estimate a maximum weight difference of about 1,4 mg, and a power of 0,9, with n.2 replicates of a complete factorial plan.

4.4 Experimental plan

Parameters were varied according to a central composite design (CCD)² that allows the estimation of quadratic effects rather than just the linear effect of the parameters on the responses. This approach is advantageous over 2^k or fractional 2^k factorial design used in the literature. For this reason, CCD designs are specially used for process optimization¹. The CCD consists of a full factorial design (2^5 experiments) with the addition of 10 axial points and 20 replicates of the centre point. The factorial and axial points were replicated two times, resulting in 104 experiments, that is $[(2^5+10) \times 2]+20=104$. The distance between the centre point and the axial points was set to 1.31. The order of the experiments was randomized to avoid the effect of systematic errors. For each run, 15 parts were produced. The parts produced in the first 5 cycles were discharged to stabilize the process, and the remaining 10 parts were considered for the analysis.

For the sake of simplicity, in the analysis we consider x as the vector of the coded process parameters (x_1, x_2, x_3, x_4, x_5), while natural variables are indicated with the name of the factor ($T_{melt}, P_{hold}, T_{mold}, v_{inj}, t_{hold}$). In Table 4.5 a summary of the variables and of the nomenclature is reported. The levels of the process parameters, with $\alpha=1.3$, are reported in Table 4.6. These levels were identified after a comparison among the suggested range of parameters reported on the material datasheet and the state of the art.

Table 4.5: Correspondence between factors, coded variables, and natural variables

Factor	Coded variables	Natural variables
Melt temperature	x_1	T_{melt} [°C]
Holding pressure	x_2	P_{hold} [bar]
Mold temperature	x_3	T_{mold} [°C]
Injection speed	x_4	v_{inj} [mm/s]
holding time	x_5	t_{hold} [s]

Table 4.6: Levels of process parameters for the experimental campaign



Levels (coded)	T_{melt} (melt temperature) [°C]	P_{hold} (holding pressure) [bar]	T_{mold} (mold temperature) [°C]	v_{inj} (injection speed) [mm/s]	t_{hold} (holding time) [s]
(+1.3)	236	1650	106	157.5	3.3
(+1)	230	1500	100	150	3
(0)	210	1000	80	125	2
(-1)	190	500	60	100	1
(-1.3)	184	350	54	92.5	0.7

The flash is a categorical variable that has been evaluated independently by three micro injection moulding experts. Even if it was possible to obtain more complex analysis of the flash defect,

² D.C. Montgomery, Design and analysis of experiments, 10th ed., John Wiley & sons, 2019.

the voting categories were simplified in 0 = no flash and 1 = flash. In case of doubtful evaluation, two out of three agreed votes assigned the category (examples extracted from the whole evaluation in Tab. 4.7).

Tab. 4.7: Example of the covariates evaluation methodologies

Run Order	Weight	Flashing	Categorical variable		
			0= no flash 1= flash	0= no flash 1= flash	0= no flash 1= flash
	[mg]	[images]	Observer 1	Observer 2	Observer 3
2	83,9		0	0	0
6	97,1		1	1	1

4.5 Dataset definition to identify the part weight and flash models

The experimental plan developed, a central composite design (Section 4.3), gives us the opportunity to observe in detail the two variables under analysis, namely the part weight, compared to which we want to optimize the process, and the flash which, being a product defect, can be considered a constrain of the part weight. We decide two different approaches to identify valuable models for both part weight and flash variables, that will be detailed in the next Chapter 5:

- a. The flash constraint has been investigated with binary logistic regression methodology using the entire CCD plan consisting of 104 experiments;
 - b. The part weight has been investigated, instead, using a reduced dataset obtained considering only the values of part weight with 0=no flash of the CCD plan and removing an outlier (run 3 in standard order due to the large residual), for a total of 70 experiments
- The CCD datasets has been used to preliminarily test the commercial simulator Autodesk Modflow®. The purpose was to evaluate its prediction capability through the percentage error model. More details on the approach used and the results obtained are given in Appendix 1.

Methodologies and tools to identify the models of part weight and flash constraint to address the optimization problem

5.1 Binary Logistic regression

Logistic regression is the statistical technique used to predict the relationship between predictors (our independent variables) and a predicted variable (the dependent variable) where the dependent variable is **binary**.

In our case, the dependent variable is the **flash** (flashing defect), introduced in Chapter 4, that has been binary categorized with **0 = no flash and 1 = flash**.

The dependent variable has been evaluated on the test parts produced with the Central composite design plan (CCD) defined in Chapter 4 Section 4.3.

In Table 5.1 is reported the Analysis of Variance of the binary logistic regression. It was adopted a stepwise approach for which are not considered all variables in the model with the p-values greater than the specified alpha to enter value (in our case alpha = 0,15) and all variables in the model with p-values less than or equal to the specified alpha to remove value (in our case Alpha = 0,15).

Table 5.1: Binary Logistic Regression in coded units

Stepwise approach with alfa=0,15			
Method			
Link function	Logit		
Rows used	104		
Stepwise Selection of Terms			
α to enter = 0,15; α to remove = 0,15			
Response Information			
Variable	Value	Count	
flashing_1	1	33	(Event)
	0	71	

Regression Equation

$$P(1) = \frac{\exp(Y')}{1 + \exp(Y')}$$

$$Y' = -3,401 + 2,285 \text{ Tmold} + 1,257 \text{ Tmelt} + 4,95 \text{ vinj} + 3,85 \text{ Phold} - 3,482 \text{ vinj} * \text{Phold}$$

Coefficients

Term	Coef	SE Coef	Z-Value	P-Value	VIF
Constant	-3,401	0,859	-3,96	0,000	
Tmold	2,285	0,582	3,93	0,000	1,95
Tmelt	1,257	0,502	2,50	0,012	1,37
vinj	4,95	1,12	4,43	0,000	5,92
Phold	3,85	1,00	3,85	0,000	4,93
thold	-3,482	0,997	-3,49	0,000	4,49

Odds Ratios for Continuous Predictors

	Odds Ratio	95% CI
Tmold	9,8255	(3,1427; 30,7193)
Tmelt	3,5161	(1,3138; 9,4105)
vinj	*	(*; *)
Phold	*	(*; *)
thold	9,8255	(3,1427; 30,7193)

Odds ratios are not calculated for predictors that are included in interaction terms because these ratios depend on values of the other predictors in the interaction terms.

Model Summary

Deviance R-Sq	Deviance R-Sq(adj)	AIC	AICc	BIC	Area Under ROC Curve
64,61%	60,76%	57,99	58,86	73,86	0,9652

Goodness-of-Fit Tests

Test	DF	Chi-Square	P-Value
Deviance	98	45,99	1,000
Pearson	98	52,16	1,000
Hosmer-Lemeshow	7	11,79	0,108

Analysis of Variance

Source	DF	Wald Test	
		Chi-Square	P-Value
Regression	5	23,82	0,000
Tmold	1	15,44	0,000
Tmelt	1	6,27	0,012
vinj	1	19,63	0,000
Phold	1	14,80	0,000
thold	1	12,19	0,000

Fits and Diagnostics for Unusual Observations

Obs	Observed Probability	Fit	Resid	Std Resid	
5	1,000	0,165	1,900	2,05	R
7	0,000	0,537	-1,241	-1,37	X
22	1,000	0,537	1,115	1,23	X
24	1,000	0,115	2,081	2,21	R
35	1,000	0,086	2,216	2,33	R
52	1,000	0,115	2,081	2,21	R
55	0,000	0,537	-1,241	-1,37	X
66	0,000	0,537	-1,241	-1,37	X
88	1,000	0,394	1,365	1,54	X
97	1,000	0,394	1,365	1,54	X

R Large residual
X Unusual X

The contour plot of Fig. 5.1 shows how flash variable relate to the process parameters based on a model equation (5.2). For each pair of parameters analysed, the area $< 0,1$ means that the probability to find flash is less than 10% (eq. 5.1). Higher values mean higher probability to find flash.

The quadratic effect of the main factors of equation (5.1) is clear for the contour plot of $Phold \cdot vinj$, the two variables that are the main cause of flash and which interaction is well balanced to demonstrate their equivalent importance.

In table 5.2 it is reported the variance covariance matrix that will be used and discussed in Chapter 6 to identify the optimal region of part weight constrained by flash.

$$P(1) = \frac{\exp(\hat{Y})}{1 + \exp(\hat{Y})} \quad (5.1)$$

$$\hat{Y} = -3,401 + 2,285 Tmold + 1,257 Tmelt + 4,95 vinj + 3,85 Phold + 3,482 vin * Phold \quad (5.2)$$

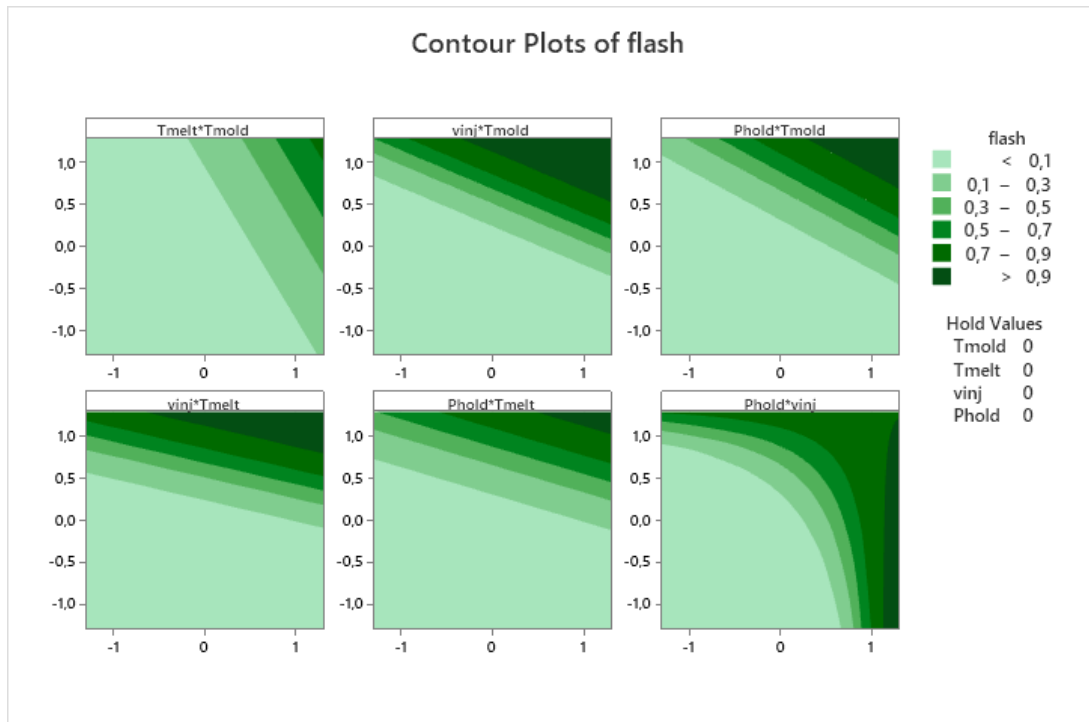


Fig. 5.1: Contour plot summary of flash variable

Tab 5.2: Variance - Covariance Matrix

0,737955	-0,158502	-0,105678	-0,80125	-0,73622	0,725698
-0,158502	0,338254	0,143945	0,33919	0,19680	-0,158366
-0,105678	0,143945	0,252291	0,15561	0,13333	-0,104554
-0,801250	0,339190	0,155613	1,24757	0,95137	-0,921081
-0,736216	0,196803	0,133329	0,95137	1,00284	-0,848643
0,725698	-0,158366	-0,104554	-0,92108	-0,84864	0,994447

5.2 Part weight model identification based on reduced dataset

In Table 5.3 it is reported the analysis of variance of the reduced model related to the part weight (eq. 5.3). The dataset used has been obtained removing from the 104 experiments of the CCD all the trials with flash=1 and an outlier, for a total of 70 experiments. Fig. 5.2 evidenced that there are no outliers and all the standardized residuals are in the range [+3; -3]. In Tab. 5.4 it is reported the variance covariance matrix that will be used and discussed in Chapter 6 to identify the optimal region of part weight.

Table 5.3 – Analysis of variance of reduced model to flash

Response Surface Regression: weight no flash versus Tmelt; Phold

Coded Coefficients

Term	Coef	SE Coef	T-Value	P-Value	VIF
Constant	88,114	0,249	353,90	0,000	
Tmelt	1,419	0,235	6,04	0,000	1,15
Phold	7,402	0,254	29,16	0,000	1,20
Phold*Phold	3,705	0,342	10,85	0,000	1,12
Tmelt*Phold	1,494	0,257	5,80	0,000	1,16

Model Summary

S	R-sq	R-sq(adj)	R-sq(pred)
1,42566	93,01%	92,58%	91,68%

Analysis of Variance

Source	DF	Adj SS	Adj MS	F-Value	P-Value
Model	4	1758,83	439,71	216,34	0,000
Linear	2	1734,82	867,41	426,77	0,000
Tmelt	1	74,19	74,19	36,50	0,000
Phold	1	1728,54	1728,54	850,44	0,000
Square	1	239,12	239,12	117,65	0,000
Phold*Phold	1	239,12	239,12	117,65	0,000
2-Way Interaction	1	68,43	68,43	33,67	0,000
Tmelt*Phold	1	68,43	68,43	33,67	0,000
Error	65	132,11	2,03		
Total	69	1890,94			

Regression Equation in Coded Units

$$\text{weight} = 88,114 + 1,091 \text{ Tmelt} + 5,693 \text{ Phold} + 2,193 \text{ Phold*Phold} + 0,884 \text{ Tmelt*Phold} \quad (5.3)$$

Fits and Diagnostics for Unusual Observations

Obs	weight	Fit	Resid	Std Resid	
2	91,767	88,114	3,652	2,60	R
5	100,600	102,134	-1,534	-1,22	X
9	102,433	102,134	0,300	0,24	X
26	102,800	102,134	0,666	0,53	X
33	99,267	96,309	2,958	2,18	R
43	103,933	102,134	1,800	1,44	X
45	87,667	84,494	3,173	2,32	R
48	81,300	84,755	-3,455	-2,55	R
52	81,500	84,755	-3,255	-2,40	R
55	85,300	88,114	-2,814	-2,00	R
69	85,200	88,114	-2,914	-2,08	R

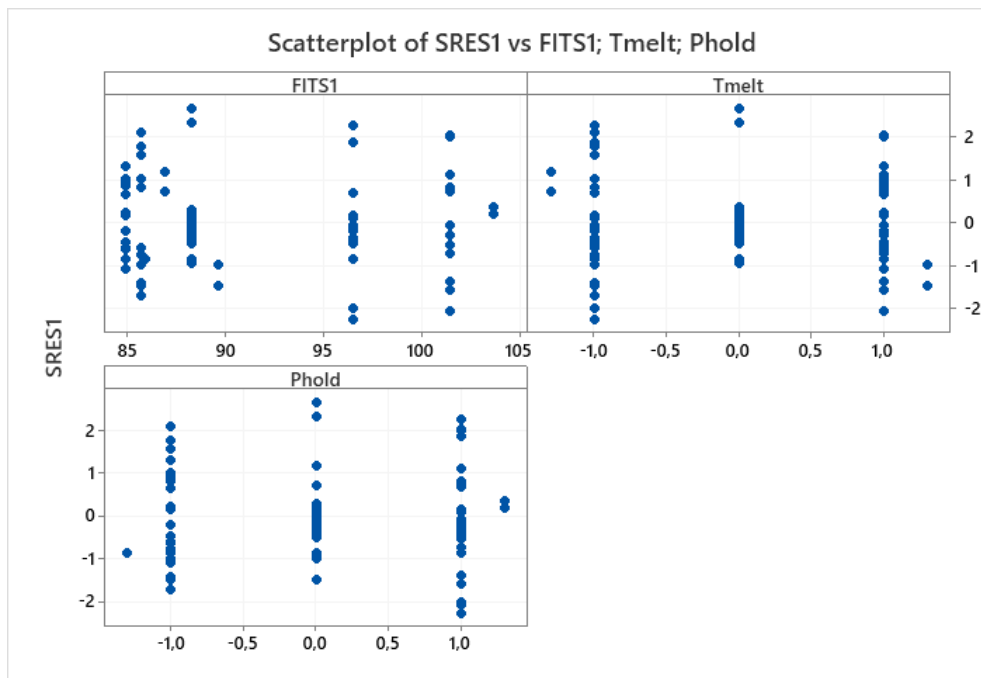


Fig. 5.2: Scatterplot of standardized residuals

Tab 5.4: Variance - Covariance Matrix

0,0619908	0,0002111	-0,0018129	-0,058998	0,0002436
0,0002111	0,0551336	0,0158097	0,014933	0,0174109
-0,0018129	0,0158097	0,0644162	0,025749	0,0182387
-0,0589980	0,0149333	0,0257492	0,116703	0,0172275
0,0002436	0,0174109	0,0182387	0,017228	0,0662791

5.3 Summary of the identified models of part weight and flash constraint

The analysis done in the previous sections has given us the opportunity to identify a part weight model (eq. 5.3) and a model of the probability of having flash (eq. 5.2), both obtained from the same experimental plan but with different datasets.

We have evidenced how flash can influence the part weight and this means that we can identify a feasible region whose boundaries are defined by the absence of flash defect.

So, the response variables used are:

1. the part weight;
2. the probability of having flash.

Let us consider that the factors evaluated are:

$$\mathbf{x} (x_1 = Tmelt, x_2 = Phold, x_3 = Tmold, x_4 = vinj, x_5 = thold)$$

Regarding the part weight, we remind that the number of significant factors is 2, so $\mathbf{x}_w = (x_1, x_2)$, and the model identified in eq. 5.3 is quadratic in two process variables:

$$\hat{w}(\mathbf{x}^w, \hat{\beta}) = 88,114 + 1,091 x_1 + 5,693 x_2 + 2,193 x_2^2 + 0,884 x_1 * x_2 \quad (5.3)$$

Model Summary

S	R-sq	R-sq(adj)	R-sq(pred)
1.42566	93.01%	92.58%	91.68%

Beta Variance - Covariance Matrix

$\hat{\beta}_0$	$\hat{\beta}_1$	$\hat{\beta}_2$	$\hat{\beta}_{22}$	$\hat{\beta}_{12}$
0,0619908	0,0002111	-0,0018129	-0,058998	0,0002436
0,0002111	0,0551336	0,0158097	0,014933	0,0174109
-0,0018129	0,0158097	0,0644162	0,025749	0,0182387
-0,0589980	0,0149333	0,0257492	0,116703	0,0172275
0,0002436	0,0174109	0,0182387	0,017228	0,0662791

Regarding the probability of having flash, the number of significant factors is 4, so $\mathbf{x}^f = (x_1, x_2, x_3, x_4)$, and the model identified with logistic regression in eq. 5.2 is reported below:

$$\mathcal{P}_F = \frac{e^{\hat{y}}}{1+e^{\hat{y}}} \text{ where } y = \hat{y}(\mathbf{x}^f, \hat{\gamma}) \quad (5.1)$$

with

$$\hat{y} = -3.401 + 1.257 x_1 + 3.85 x_2 + 2.285 x_3 + 4.95 x_4 - 3.482 x_2 x_4 \quad (5.2)$$

γ Variance covariance Matrix

γ_0	γ_1	γ_2	γ_3	γ_4	γ_{24}
0,737955	-0,158502	-0,105678	-0,80125	-0,73622	0,725698
-0,158502	0,338254	0,143945	0,33919	0,19680	-0,158366
-0,105678	0,143945	0,252291	0,15561	0,13333	-0,104554
-0,801250	0,339190	0,155613	1,24757	0,95137	-0,921081
-0,736216	0,196803	0,133329	0,95137	1,00284	-0,848643
0,725698	-0,158366	-0,104554	-0,92108	-0,84864	0,994447

If we impose a maximum probability of having a flash we have:

$$\widehat{\mathcal{P}}_F(\mathbf{x}^f, \hat{\gamma}) \leq \alpha \rightarrow \hat{y}(\mathbf{x}^f, \hat{\gamma}) \leq \ln\left(\frac{\alpha}{1-\alpha}\right) = k_0 \quad (5.4)$$

So, for example we can have:

α	k_0
0.01	-4.595
0.05	-2.944
0.10	-2.197
0.50	0.000

**Optimization problem:
procedure, results and discussion**

6.1 Introduction

In this chapter is presented the procedure, based on bootstrap simulation and data depth, used to identify a confidence region for the optimum of weight subjected to the constraint of the probability of flash.

The procedure is based on the experimental approach described in the previous chapter and whose models are summarized below.

The vector $\mathbf{x} = \{x_1, x_2, x_3, x_4, x_5\}$ reported in fig. 6.1 is the vector of the main process parameters, namely $x_1 = T_{melt}$, $x_2 = P_{hold}$, $x_3 = v_{inj}$, $x_4 = T_{mold}$, $x_5 = t_{hold}$, preliminary identified to built the experimental plan.

A logistic regression model was estimated to describe the probability of flash formation as function of the most significant process parameters. The model is:

$$\mathcal{P}_f = \frac{e^{\hat{y}}}{1 + e^{\hat{y}}}$$

where

$$\hat{y}(\mathbf{x}^f, \hat{\boldsymbol{\gamma}}) = -3.401 + 1.257x_1 + 3.85x_2 + 2.285x_3 + 4.95x_4 - 3.482x_2x_4 \quad (6.1)$$

where

$$\hat{\boldsymbol{\gamma}} = (-3.401, 1.257, 3.85, 2.285, 4.95, -3.482)$$

and

$$\mathbf{x}^f = \{x_1, x_2, x_3, x_4, \} \text{ with } x_1 = T_{melt}, \quad x_2 = P_{hold}, \quad x_3 = v_{inj}, \quad x_4 = T_{mold}$$

The constraint can be rewritten in a linear form considering the following relationship:

$$\mathcal{P}_f \leq \phi \rightarrow \hat{y}(\mathbf{x}^f, \hat{\boldsymbol{\gamma}}) \leq \ln\left(\frac{\phi}{1 - \phi}\right) = k_0$$

Where \mathbf{k}_0 is related to the probability of flash formation ϕ .

The conditions of the full experimental plan (CCD plan with $N=104$) that did not result in flash formation ($NR=70$), were used to estimate the weight of the parts as function of the most significant process parameters. The regression equation is the following:

$$\hat{w}(\mathbf{x}^w, \hat{\beta}) = 88.114 + 1.091x_1 + 5.693x_2 + 2.193x_2^2 + 0.884x_1x_2 \quad (6.2)$$

where

$$\hat{\beta} = (88.114, 1.091, 5.693, 2.193, 0.884)$$

and

$$\mathbf{x}^w = \{x_1, x_2\} \text{ with } x_1 = T_{melt}, x_2 = P_{hold}.$$

6.2 Optimization Procedure

Step 1

The step 1 (fig. 6.1) of the procedure is the estimate of the objective and constraint function based on experimental data. The weight function $\hat{w}(\mathbf{x}^w, \hat{\beta})$ is described by the linear regression model eq.(6.1), while the constraint $\hat{\mathcal{P}}_F(\mathbf{x}^f, \hat{\gamma})$ is described by the binary logistic regression model eq.(6.2).

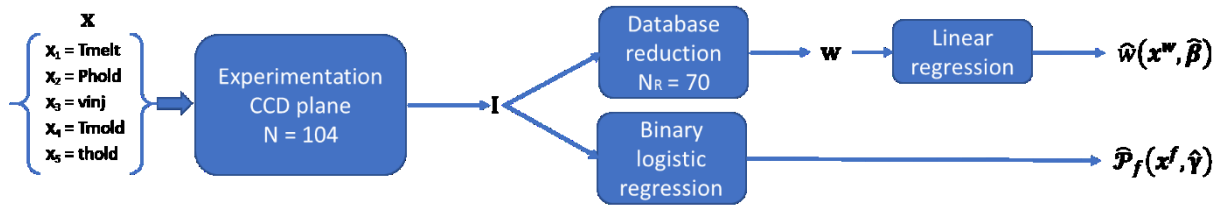


Fig. 6.1: Workflow of the step 1 of the procedure: experimentation

Step 2

In step 2 the bootstrap simulation has been used [1, 2]. The bootstrapping procedure proposed in [1] has been implemented using the original dataset I (fig. 6.1). Each bootstrap produces the vector I_i of $\{0, 1\}$. The bootstrap procedure produced a matrix of NB column and N strings that has been processed by binary logistic regression obtaining NB sets of $\hat{\gamma}^B$. For each bootstrap I_i , the conditions that resulted in a lack of flash defect were used to create a subset column of $\{1\}$ and considered for bootstrapping the weight function. The result of bootstrapping the weight function with the vector of NRi strings (with $N > NRi > 0$) and NB columns are NB sets of $\hat{\beta}^B$. This procedure has been selected to mimics the experimental approach used to estimate eq. (6.1) and eq. (6.2).

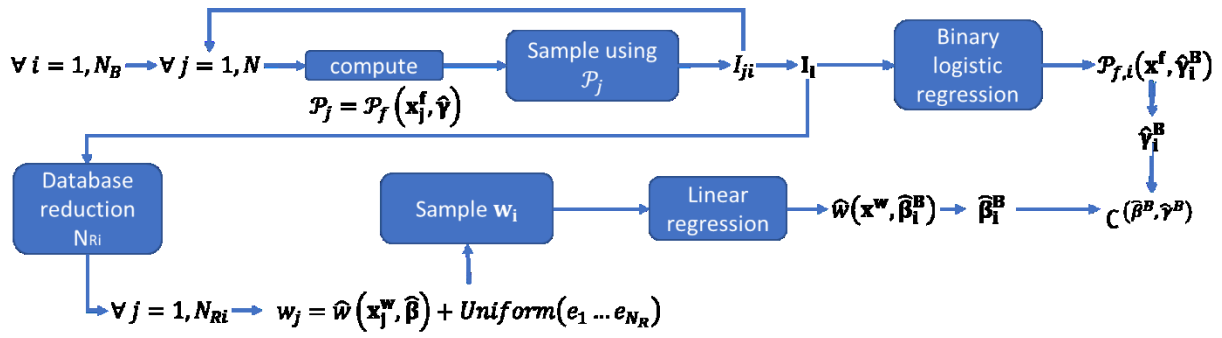


Fig. 6.2: workflow of the step 2 of the procedure: bootstrapping

Step 3

In Step 3, projection data depth [3] is used to order the NB instances of the bootstrap results. The NB instances $[\hat{\beta}^B, \hat{\gamma}^B]$ were ordered by trimming the $\alpha\%$ outermost [3-9]. So, the confidence region $C^{(\hat{\beta}^B, \hat{\gamma}^B)}$ (fig. 6.2) identified after bootstrapping is reduced to the new confidence region $C_{1-\alpha}^{(\hat{\beta}^B, \hat{\gamma}^B)}$ (Fig.6.3), that indicates the confidence region of the coefficients of the models in eq. (6.1) and eq. (6.2).



Fig. 6.3: workflow of the step 3 of the procedure: trimming

Step 4

In step 4 the optimization problem has been solved using a utility function (eq. 6.1) that is defined as the product between the weight of the part and the probability of flash formation for each set of process parameters (x) and for each bootstrapped set of parameters. The utility function is the following:

$$u(x^*, \hat{\beta}_i^B, \hat{\gamma}_i^B) = w(x^w, \hat{\beta}_i^B)(1 - P_F(x^f, \hat{\gamma}_i^B)) \quad (6.3)$$

If the probability of flash formation is large (that eq. (6.1) is close to 1), then the value of $u(x, \hat{\beta}_i^B, \hat{\gamma}_i^B)$ becomes close to 0 for every value of the part weight, and this means that are avoided the regions of the parameters where the defect probability is large independently from the value of the weight function. When the probability of flash formation is close to 0, instead, the utility function is comparable to the weight function.

Step 5

In Step 5 the optimality criteria for process optimization is selected. The utility function must be maximized; however, there are as many utility functions as the result of the trimming procedure, that is equal to NB $(1-\alpha)$. The values of the coefficients $\hat{\beta}^B$ influence the weight of

the part, while the coefficients $\hat{\gamma}^B$ define the position of the constraint in the region of the parameters.

This means that for a specific combination of input parameters x^* , there are NB $(1-\alpha)$ values of the utility function. So, for the selection of the optimality region some statistics are used to describe the value of $u(x^*, \hat{\beta}_i^B, \hat{\gamma}_i^B)$ at each point x^* :

- Median
- 5th quantile
- Mean

These indexes have been selected because they better describe than others (Maximum, standard deviation, etc.) how the utility function behaves in the region of the parameters x^* .

6.3 Results and discussion

6.3.1 Optimal value of part weight under deterministic constraint

The optimization problem has been preliminary solved considering the probability of flash formation as deterministic constraint. Starting from the Step 1 of Section 6.1, once defined the probability of flash formation model and the part weight model, we maximized the utility function of eq. 6.3 to find the optimal set of parameters $x_{0,D}^*$ (fig. 6.3). When the probability of flash formation is close to 0, the utility function maximizes the weight of the part, which is a proxy of a successful filling phase. In the processing conditions that have a non-zero probability of flash formation, the weight is “penalized” and the utility is reduced. Therefore, the region where the flash formation is expected results in a lower utility.

The optimization was carried out in the range $[-1;1]$ even though the parameters were varied in the range $[-1.3; 1.3]$. This choice was made because in the limited range $[-1;1]$ the variance of the predicted response is minimized [10] allowing a robust selection of the optimal conditions.

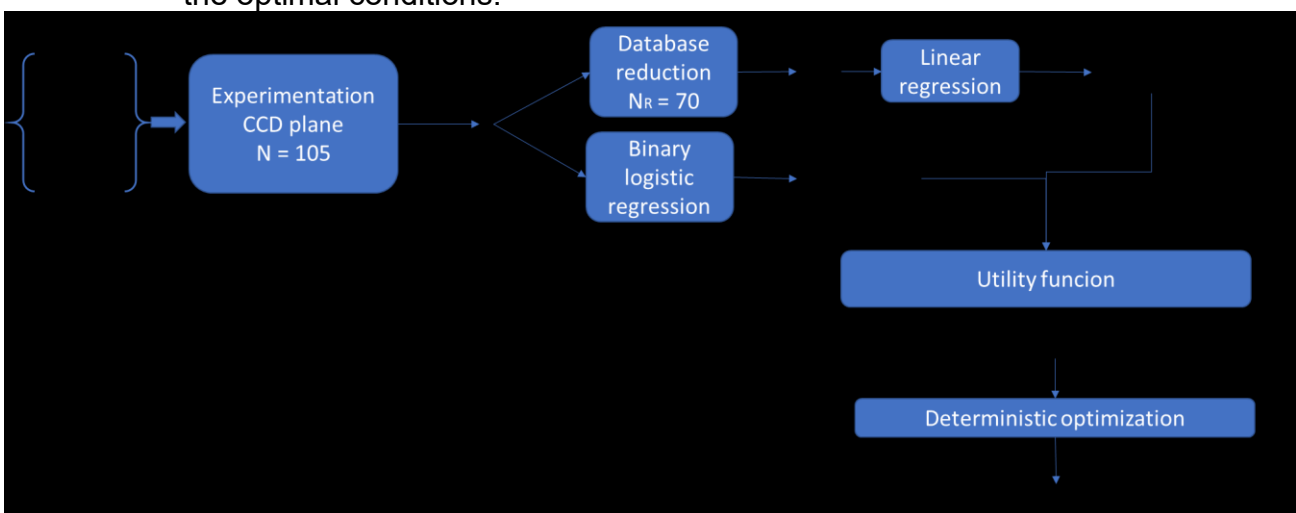


Fig. 6.3: workflow to solve the deterministic optimization problem using the utility function of eq. 6.3

The utility function in Eq (6.3) was used to identify the optimal processing conditions that are the combinations of Phold, Tmelt, Tmold and vinj that maximize the weight. The utility function in Fig. 6.4 is plotted against Phold and Tmelt while Tmold = vinj = -1. Utility increases as Phold and Tmelt increase, however as these two variables approach 1, the utility sees a sharp decrease. The reduction in the utility is due to the increased probability of flash formation, as shown in Figure 6.5.

The maximum utility (93.54) is achieved at Tmelt=1, Phold=0.7, and Tmold=vinj=-1 as reported in Table 6.

Table 6: Optimal process parameters based on the maximization of the utility function

Optimal processing conditions Coded variables					Optimal processing conditions Uncoded I variables					Weight (mg) $x_{0,D}^*$	Flash probability
T _{melt} [°C]	P _{hold} [bar]	T _{mold} [°C]	V _{inj} [mm/s]	t _{hold} [s]	T _{melt} [°C]	P _{hold} [bar]	T _{mold} [°C]	V _{inj} [mm/s]	T _{hold} [s]		
1	0.7	-1	-1	-1	230	1350	100	150	1	94.9	1.4%

Tmold and vinj should be set at their lowest level because, in this condition, the probability of flash formation is minimized, and they do not influence the weight of the part. On the contrary, Tmelt should always be set at the highest level because it maximizes the weight of the part. Holding time (thold) does not affect the weight nor the flash probability, so it is set at the values that maximizes the productivity of the process; that is thold = 1 s. As previously noted, the minimization of the probability and the weight maximization are opposite objectives in terms of process parameters selection. To maximize weight, Phold and Tmelt should be maximized. However, at the same time, this choice leads to the maximization of the flash formation probability. There is a wide region of parameters that ranges from Tmelt [-1;1] and Phold [0.5; 1] that shares similar values of utility with the optimal values. This region is indicated by red contour lines in Fig. 6.5.

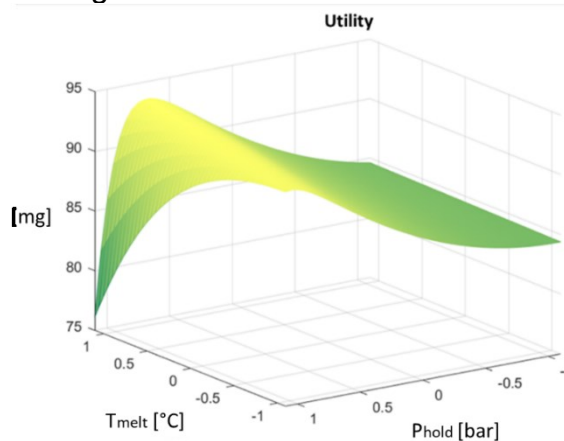


Fig. 6.4: Utility as function of Phold and Tmelt (vinj = Tmold = -1)

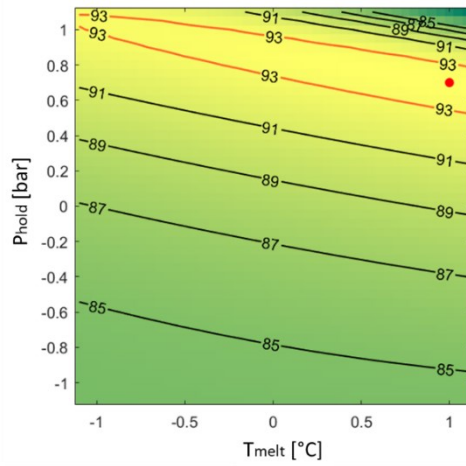


Fig. 6.5: Contour plot of the utility function. The red dot indicates the optimal processing condition.

Optimizing processing conditions in μIM requires a compromise between maximizing weight and minimizing the likelihood of producing components with flash. The optimal point involves a reduction of the holding pressure, which results in lower pressure on the cavity of the mould with a consequent reduction in the risk of reaching the limit of the clamping force. Therefore, a high temperature of the molten polymer must be used to reduce viscosity to correctly fill the microcavity and, at the same time, to compensate for the pressure reduction.

6.3.2 Optimal region of part weight under stochastic constraint

Analyzing eq. (6.1), we can see that if $\hat{\gamma}_4$ (coefficient of x_3) is positive and if $\hat{\gamma}_6$ (coefficient of the interaction x_{24}) is negative, then the solution of the optimization problem requires that $x_3 = -1$ and $x_4 = -1$. In fact, if we look at the NB bootstrapped coefficients of Fig. 6.6, we can see that, for all the vectors of the bootstrapping procedure, the $\hat{\gamma}_4$ coefficient is always positive and the $\hat{\gamma}_6$ coefficient is always negative. So, to minimize the probability of flash formation T_{mold} and vinj must be set at their lowest level.

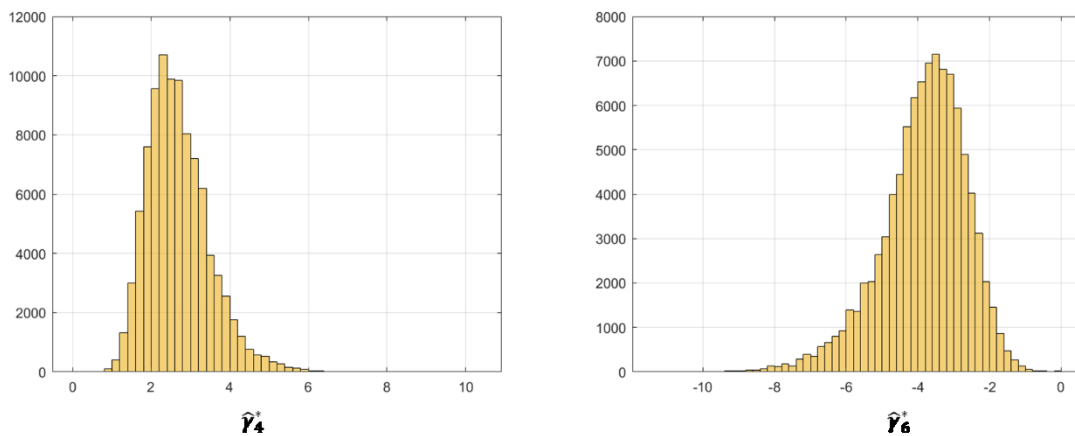
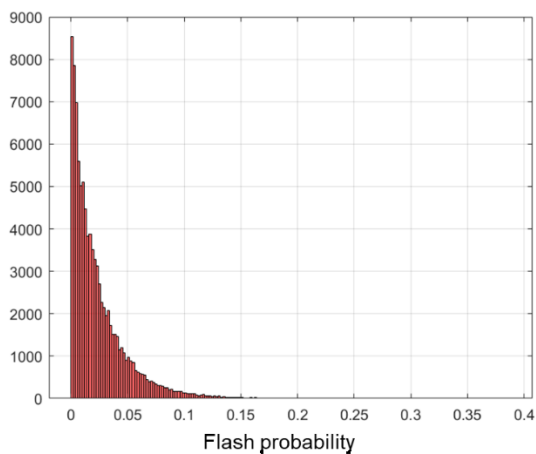


Fig. 6.6: B bootstrapped values of the coefficients of T_{mold} , $\hat{\gamma}_4$, and the coefficient of the interaction $\text{vinj} \cdot \text{Phold}$, $\hat{\gamma}_6$

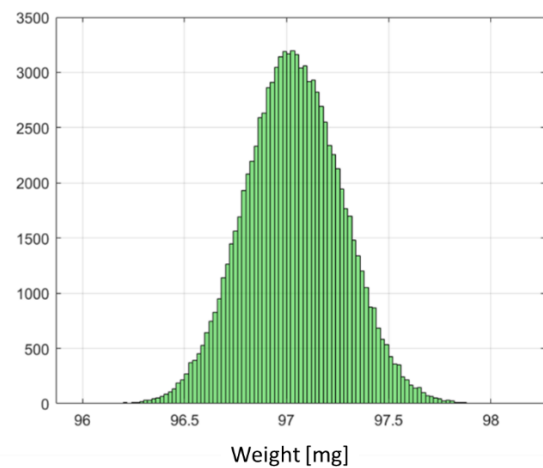
So, the optimization problem can be focused only on the optimization of x_1 (T_{melt}) and x_2 (P_{hold}) because they both influence the objective function and the constraint. In detail, as T_{melt} and P_{hold} increase the weight increases (and therefore the quality), but at the same time also the defect probability increases. The utility function can help to find a compromise between these two conflicting aspects.

For each combination of $(x_1, x_2) = (T_{melt}, P_{hold})$ B bootstrapped values of weight and flash probability were generated in Step 4, 5% of which were trimmed, resulting in 95000 values. For clarity purposes, the distribution of the weight and probability of flash formation for a selected point are shown in Figure 6.7 (the point is $x_1 = 0.8$ and $x_2 = 0.8$).

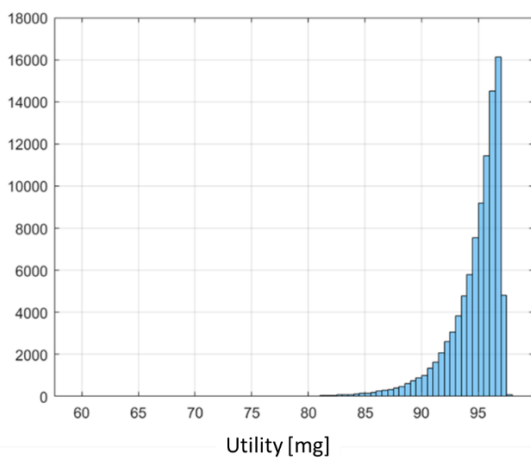
The probability of flash formation varies between 0 and 0.4 (fig. 6.7a), as expected because as T_{melt} and P_{hold} increase the defect probability also increases. However, around 8500 simulations resulted in a lack of formation of flash which is little less than 10% of the overall generated data. The weight distribution follows a gaussian distribution centered in 97 mg (fig. 6.7b). The resulting utility function for this specific combination of parameters is shown in Figure 6.7c. The utility has a right-skewed distribution due to the shape of the flash probability in Figure 6.7a.



a)



b)

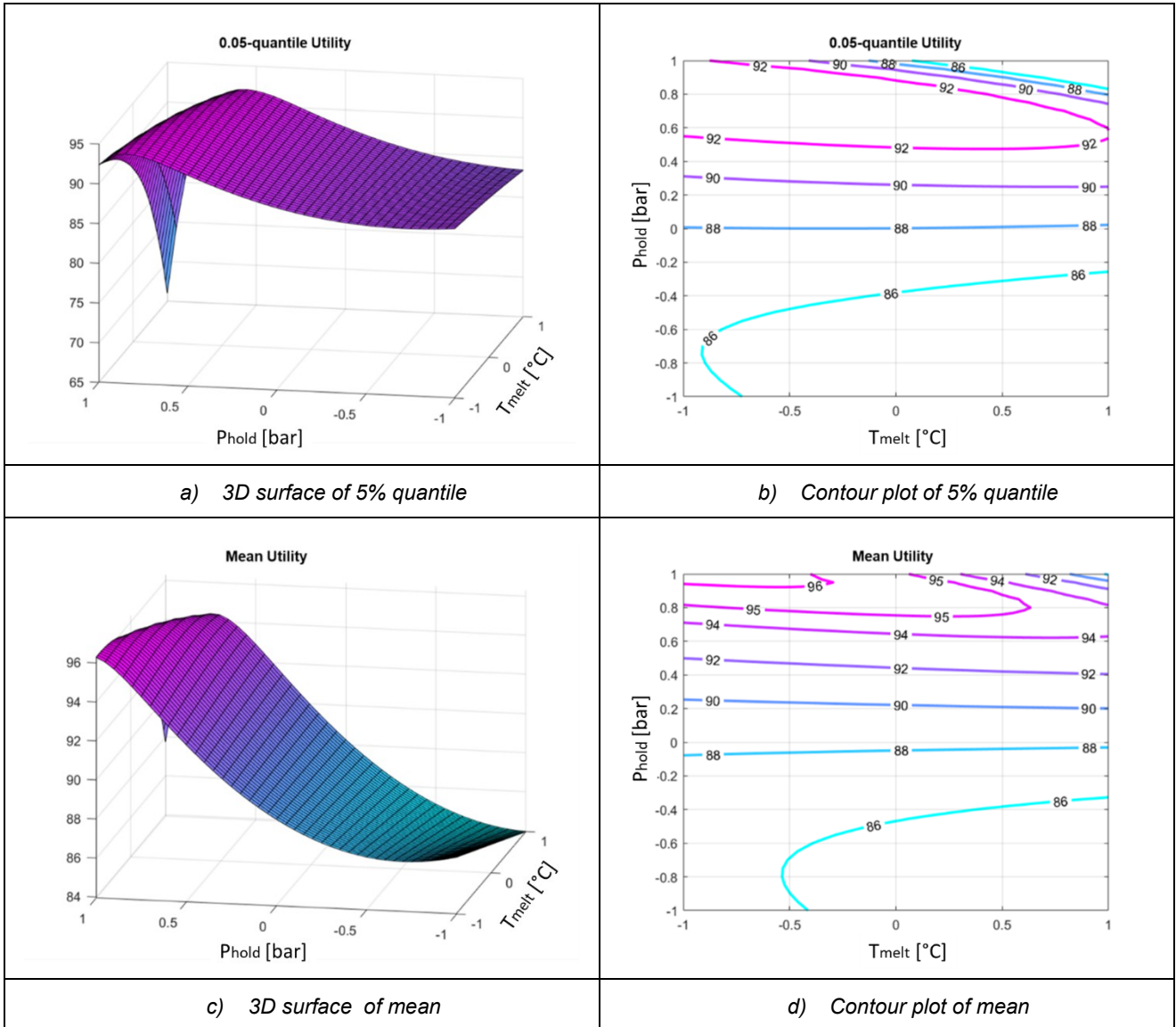


c)

Fig. 6.7: Examples of distributions of flash probability (a), weight (b), and utility function (c) for a specific point in the region of the parameters. In this case $x_1=t_{melt}=0.8$ and $x_2=Phold=0.8$.

For the specific case in Fig. 6.7 **Errore. L'origine riferimento non è stata trovata.**, the mean utility is 94.7 mg, the median is 95.4 mg and the 5% quantile is 89.78 mg. The mean and median utility show closer values, while the 5% quantile of the utility function has lower values because it is more conservative.

Considering the indexes reported at Step 5, the resulting utility functions are shown in the following Fig. 6.8.



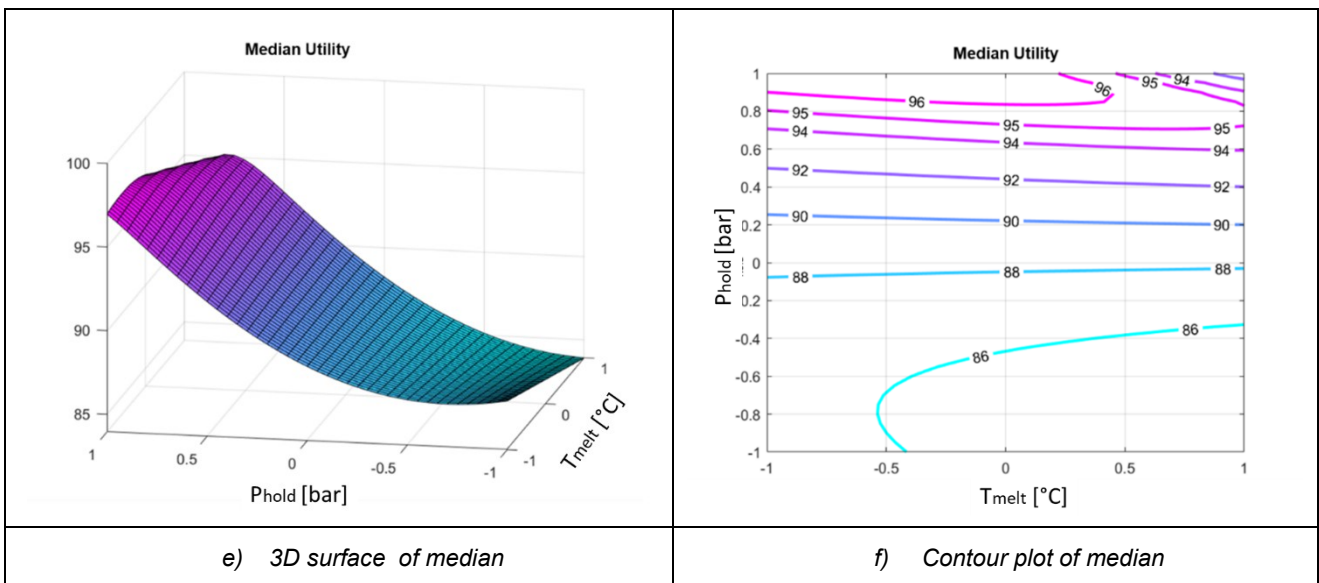


Figure 6.8: Utility functions based on different indexes. a) 0.05-quantile, b) mean and c) median

The shape of the three utility functions in **Errore. L'origine riferimento non è stata trovata.** is mostly the same, in particular for mean and media, while the 5% quantile is more conservative. If we look at the contour plots of fig. 6.8 b, d, f, we can observe that at low levels of both parameters ($Phold$ and T_{melt}), the utility values are low because of the low weight of the part. At the same time in the same evaluated region, the probability of flash formation is close to 0. As $Phold$ (x_2) increases, the utility also increases reaching its maximum when $Phold$ is larger than 0.8. However, in the upper right corner ($x_1 = x_2 = 1$) there is a sharp decrease in the utility mostly due to the high probability of defect formation. Median and Mean utility function reach the same maximum value of 96, while the maximum value of the 5% quantile utility function is 92 and therefore lower, as expected, because choosing the 5% quantile means to select the value of utility that is exceeded by 95% of the values. On the contrary, mean and median allow for an increased utility accepting a higher risk of defects for the parts. Since the distribution of the utility (Fig. 6.7) is not symmetrical, the median index is preferred to the mean. An overimposition of the optimal region for the 5% quantile of utility and median is shown in Fig. 6.9 where in yellow it is evidenced the optimality region for micro injection moulding.

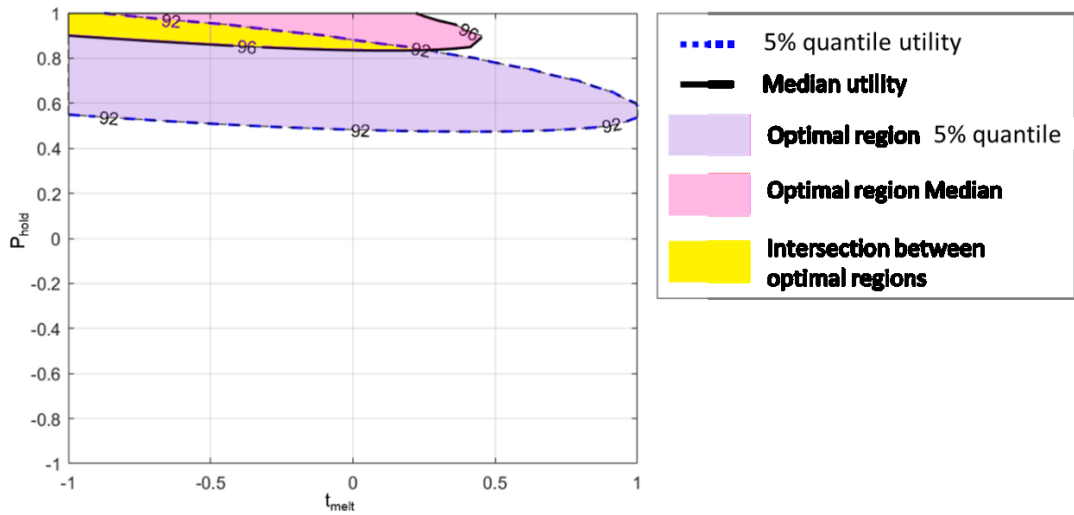


Figure 6.9 - Optimality region (yellow) for the micro-injection process.

6.4 Nomenclature

Symbol	Definition	Value
\mathbf{x}	Vector of the main process parameters	See Fig. 6.1
\mathbf{x}^f	Vector of the most significant process parameters of the to describe the probability of flash formation	See eq. (6.1)
\mathbf{x}^w	Vector of the most significant process parameters of the weight model	See eq. (6.2)
\mathbf{x}^*	Vector of the most significant process parameters of the utility function	See eq. (6.3)
\hat{y}	Estimated logistic equation for flash formation probability based on experimental data	See eq. (6.1)
\hat{w}	Least square estimate of the weight of the part based on experimental data	See eq. (6.2)
N	Combination of process parameters of the full CCD plan	
N_R	Reduced database of N that did not result in flash formation	
N_B	Combination of process parameters of the Bootstrap sampling of the logistic model that did not result in flash formation	
N_{Ri}	Combination of process parameters of the Bootstrap sampling of the logistic model that did not result in flash formation	
i index	$i \in \{1, N_B\}$	
j index	$j \in \{1, N\}$	
$\hat{\beta}^B$	Bootstrap coefficient of the weight function	
$\hat{\gamma}^B$	Bootstrap coefficient of the constraint function	
$\hat{\beta}$	Coefficient of the experimental weight function	
$\hat{\gamma}$	Coefficient of the experimental constraint	
α	Percentage of trimmed data	5%
B	Number of iterations of the bootstrap procedure	100000

6.5 References

- [1] Adjei, I. A.; Karim, R. (2016), An application of Bootstrapping in Logistic Regression Model, *Open Access Library Journal*, 3: e3049, <http://dx.doi.org/10.4236/oalib.1103049>;
- [2] del Castillo, E.; Chen, P.; Meyers, A.; Hunt, J.; Rapkin, J. (2020), Confidence regions form the location of response surface optima: The R package *OptimaRegion*, *Communications in statistics-Simulation and Computation*, <https://doi.org/10.1080/03610918.2020.1823412>.
- [3] Pokotylo, O.; Mozharovskyi, P.; Dyckerhoff, R. (2019), Depth and depth-based classification with R-package *ddalpha*, *Journal of Statistical Software*, 91, 1 – 46;
- [4] Lange, T.; Mosler, K.; Mozharovskyi, P. (2014), Fast nonparametric classification based on data depth, *Statistical Papers*, 55, 49–69.
- [5] Lange, T.; Mosler, K.; Mozharovskyi, P. (2014), $DD\alpha$ -classification of asymmetric and fattedata, In: Spiliopoulou, M.; Schmidt-Thieme, L.; Janning, R. (eds), *Data Analysis, Machine Learning and Knowledge Discovery*, Springer (Berlin), 71–78.
- [6] Mosler, K.; Mozharovskyi, P. (2017), Fast DD -classification of functional data, *Statistical Papers*, 58, 1055–1089.
- [7] Mozharovskyi, P. (2015), *Contributions to Depth-based Classification and Computation of the Tukey Depth*, Verlag Dr. Kovac (Hamburg).
- [8] Mozharovskyi, P.; Mosler, K.; Lange, T. (2015), Classifying real-world data with the $DD\alpha$ - procedure, *Advances in Data Analysis and Classification*, 9, 287–314.
- [9] Nagy, S.; Gijbels, I.; Hlubinka, D. (2017), Depth-based recognition of shape outlying functions, *Journal of Computational and Graphical Statistics*, 26(4), 883-893.
- [10] Montgomery DC. (2019), *Design and analysis of experiments*, John Wiley & Sons, 10th ed.

CHAPTER 7

Conclusions

The present work focused on the evaluation of part weight as an affordable variable to be easily implemented in an industrial environment to estimate the quality of the moulded part.

The quality of the produced components in μ IM process is still an open question to which researcher are still trying to give an answer. Some defects, such as flash formation, are more usual than standard injection moulding due to the extreme process conditions of the micro injection moulding process and arise when the part weight is maximized.

In the proposed work, it has been defined a procedure to identify an optimality region for the maximum weight of the moulded part in which the risk of generating flash is minimized.

For the first time, such a procedure was applied to a technological problem and, additionally, the procedure was generalized to also consider a stochastic constraint.

An extensive experimental campaign based on a Central Composite Design CCD was carried out to assess the influence of five process parameters (namely holding pressure, molding temperature, injection speed, holding time and melting temperature)

These parameters have been chosen based on the available literature to easily verify the effectiveness of the proposed method and the further steps forward compared to the state of the art. It was decided, for example, to set the injection pressure at the maximum level allowed by the machine and vary the injection speed. This approach, which tends to minimize the cycle time, is certainly more useful from an industrial point of view. Further insights into the topic of cycle time could introduce additional factors related to the dynamics of the press, in terms of performance. In this sense, for example, the analysis of the switchover point could be a factor able to give interesting indications on the precision of the machine because its variability can introduce more or less material in the cavity and concretely affect the part weight.

Flash formation has been evaluated by three injection molding experts that provides a binary response to determine if flash is formed, 1= flash and 0=no flash. This approach is replicable in an industrial environment where the presence of defects should be assessed instantly, however it has limitations because different

levels of severity of flash can be determined. Even if the methodology proposed is not affected by this simplification, a future step will consider the opportunity to extend to more than two levels the flash evaluation. In this way, we expect to have a much broader and more precise evaluation criteria.

The experimental data were used to estimate two regression models: a quadratic model describing the weight of the component, affected by melt temperature and holding pressure, and a logistic model for the probability of flash formation, that is influenced by the same parameters as the weight and in addition by mould temperature and injection speed.

The selection of the optimal level of the process parameters was carried out using a utility function.

The utility function aims at finding a compromise between the maximization of the weight and the minimization of the probability of flash formation.

The constrained optimization problem has been previously solved with the deterministic approach, and the optimal point obtained involves a reduction of the holding pressure, which results in lower pressure on the cavity of the mould with a consequent reduction in the risk of reaching the limit of the clamping force. Therefore, a high temperature of the molten polymer is necessary to reduce the viscosity to fulfill the microcavity and, at the same time, to compensate for the necessary pressure reduction to prevent flash formation.

Then the constrained optimization problem has been solved considering a stochastic constrain. The bootstrap technique and data depth approach has been used to identify the optimality region of the part weight constrained by the region related to the probability of flash formation. The results evidenced how effective the proposed approach is than the deterministic one. An overimposition of the optimal region for the 5% quantile of utility and median, evidenced the optimality region for micro injection moulding.

The result of this novel approach is a greater variability of the main process parameters, namely T_{melt} and P_{hold} , and this means a greater variability of the micro injection moulding process without falling into the risk of producing waste parts.

The use of a utility function that correlates two variables of the same process has proved to be fundamental for the construction of the optimality region. An approach based on the use of a utility function can be extended to other related parameters and defects, as well as being applied to the study of further process-related aspects, such as an energy-based utility approach, or on the convenience or not of some types of geometries that could increase the occurrence of problems related to the material shrinkage, for example.

Future steps will involve also a simulation approach in order to have more predictive ability. Preliminary results related to the comparison of process simulation and experimentation are given in Appendix 1. It has been defined a procedure for correctly setting the simulator parameters in order to minimize the percentage error related to the part weight and consequently to improve the ability of the simulator to predict the flash formation.

Part weight comparison between simulation and experimentation: preliminary analysis

A1.1 Introduction

A part of the Phd activity focused on the study of the simulation process of micro injection molding and in particular on the identification of the intrinsic parameters of the simulator whose setting may affect the part weight.

The choice of the part weight, as observed variable, is linked to the need for a variable easily measurable and therefore that can provide a fast response on the quality of the component.

The part weight is widely used for classic molding, as discussed in previous chapters, while it is the subject of study in the field of micro injection molding technology, among others, which is not yet properly exploited precisely because of the difficulty of measuring its miniaturised components and the scarcity of measuring and simulation tools that it can provide, as is the case with classical moulding, a valid support both for the designer and for the production.

Therefore the activity proposed with the doctorate fits into this gap with the clear intention of trying to build a new procedure for the analysis of the micro injection moulding process, which uses on the one hand the process parameters configurable on the machine and, on the other hand, trying to identify, within the thermoplastic simulation software Autodesk Moldflow[®], which parameters can have a greater influence on the part weight in order to identify a prediction model on the basis of which you can try to optimize the process and have a clearer vision of how different the approach to the micro world is compared to the macro; and so what factors need to be "calibrated" for a correct prediction of the process in order to minimize waste and then make micro injection molding process more repeatable and therefore more reliable.

A1.2 Simulator parameters

The simulator parameters identified that can influence the part weight are:

Heat Transfer Coefficient (HTC): defines the heat transfer at the interface between the molten polymer and the mould wall, which models the associated thermal resistance. If $HTC = 0$, there is no heat exchange between molten polymer and mould. The higher the HTC value, the greater the heat transfer from molten polymer to mould. The HTC values are set at different values for filling, packing and cooling analysis in a proportional way so that once the temperature reduces, due to the cooling of the material, the HTC value is reduced too.

The cooling conditions under which the melt is injected, cooled and packed also need to be considered. The heat transfer coefficient in μ IM is more difficult to determine because it has a stronger dependence on pressure, melt viscosity, part shrinkage as well as newly emerged factors such as the wall slip phenomenon. One approach to obtain the heat transfer coefficient involves measuring the heat flux and the melt/mold temperatures at the interface via experimental methods. Alternatively, comparing simulation results with short-shot experiments to get a best fit also allows us to obtain heat transfer coefficients comparable to those directly found in experiments. However, in both methods the heat transfer coefficient in μ IM is considered as a constant, which neglects its process condition dependence. Instead, a variable heat transfer coefficient seems to be more applicable in predicting the polymer filling in micro-channels. Furthermore, in most existing numerical simulations (for both CIM and μ IM), the material is treated as an incompressible flow during the filling phase, indicating the neglect of the melt compressibility effects. Under extremely high pressure as in μ IM, the rarely considered melt compressibility may produce significant influence on parameter predictions. As demonstrated in a recent report, failure to consider melt compressibility apparently underestimates the filling pressure, especially at the late stage of the melt filling process, and as a result, this gives inaccurate information on the part density. To overcome this defect, the compressibility (i.e., the nonzero term, $\partial\rho/\partial t$) should be included in the continuity equation as applying simulations.

Coefficient of Thermal Expansion (CTE): is a material property which characterizes the ability of a plastic to expand under the effect of increasing temperature. It tells us how much the developed part will remain dimensionally stable under temperature variations. Two values representative of the transversally isotropic CTE are considered: Alpha 1 (Coefficient of thermal expansion in the flow direction) and Alpha2 (Coefficient of thermal expansion in the transverse direction).

Cross WLF viscosity model: is the viscosity model typically used in numerical softwares for injection moulding because, compared to other models such as Ellis, Bird-Careau, etc., describes the temperature, shear rate, and pressure dependant of the viscosity.

The viscosity model is given by the following equation:

$$\eta = \frac{\eta_0}{1 + \left(\frac{\eta_0 \dot{\gamma}}{\tau^*}\right)^n} \quad (\text{A1.1})$$

where:

η is the melt viscosity (Pa s)

η_0 is the zero shear viscosity or the 'Newtonian limit' in which the viscosity approaches a constant at very low shear rates,

$\dot{\gamma}$ is the shear rate (1/s)

τ^* is the critical stress level at the transition to shear thinning, determined by curve fitting, and

n is the power law index in the high shear rate regime, determined by curve fitting.

The zero shear viscosity is given by the equation:

$$\eta_0 = D_1 \left[-\frac{A_1(T-T^*)}{A_2+(T-T^*)} \right] \quad (\text{A1.2})$$

where

- T is the temperature (K)
- T^* is the glass transition temperature, determined by curve fitting,

$$A_2 = A_3 + D_3 p$$

- p is the pressure (Pa),

and where

- D_1, A_1, A_3 and D_3 are data-fitted coefficients.

The glass transition temperature is given by the equation: $T^* = D_2 + D_3 p$ where D_2 is a data-fitted coefficient.

Among all the parameters observed, D_1 can be considered the most influential because can significantly affect η_0 , and consequently η .

A1.3 Variability range of simulator parameters

The identification of the range of the simulation parameters was one of the most critical aspects because it was necessary to identify a range that could affected the part weight but without leading to divergence the simulator.

A preliminary screening was done but the ranges identified were not large enough to detect their influence on the part weight. An expert of Autodesk Moldflow has been consulted in order to understand with which criterion to choose the range of the simulator parameters identified. The following Table A1.1 is a summary of the assessments done.

Table A1.1 - preliminary ranges of the simulator parameters

	Process parameters					Software parameters				
	Tmold [°C]	Tmelt [°C]	vinj [mm/s]	Phold [bar]	thold [s]	viscosity (D1)	HTC filling [W/m ² -C]	HTC packing [W/m ² -C]	HTC detached [W/m ² -C]	CTE
low (-)	60	190	100	500	1	5,13714E+14	1500	850	400	0,00005
high (+)	100	230	150	1500	3	9,54034E+14	15000	7500	3750	0,00050

the reason that viscosity did not appear to a significant factor is because the level of change was lower than the other parameters?

we don't have a good range of values for the HTC coefficients from which to draw a similar high-low range

This factor mostly influences final part dimensions and shrinkage, but will have no influence on the weight

suggestions

a reasonable way to set these levels is to look at the range of typical values in the similar class of materials and processes. (For example, to make a search on typical CTE values of all unfilled POM grades in our database and use this range to set the high and low thresholds).

According to the analysis of table A1.1, for each one of the simulator parameters different criteria has been used:

- The HTC parameter is splitted, on the software in n.3 subparameters, namely HTC filling, HTC packing ed HTC detached. We decide to set them with the same variability defined for the screening tests and in agreement with the Moldflow expert, considering that the parameter HTC filling loses significance if it is set too near to the extreme values 0 [W/m² °C] and 20,000 [W/m² °C]. For HTC packing and HTC detached, instead, once defined the interval for HTC filling, it has been used the same proportion proposed by Moldflow, so halving HTC filling values to have HTC packing values, and then halving HTC packing values defined to have the HTC detached values.
- As regards D1, we decided to apply the approach proposed by the Moldflow expert. So, thanks to a specific search criterion for the D1 parameter available in Moldflow material database, it was possible to query the database to identify the maximum and the minimum value of D1 among all the POM available.
- The same approach has been used also for CTE. After a check on the available database for POM, from which it emerges that quite all the alpha values are set equal, we decide to use the extreme values that haven't given problem of divergence during simulations.

In Table A1.2 are reported the levels of the process parameter defined for the experimental campaign (Chapter 4) and the levels of simulator parameters to be tuned in the simulator.

Table A1.2 - Ranges of the simulator parameters identified

	Process parameters					Software parameters				
	Tmold [°C]	Tmelt [°C]	vinj [mm/s]	Phold [bar]	thold [s]	viscosity (D1)	HTC filling [W/m^2-C]	HTC packing [W/m^2-C]	HTC detached [W/m^2-C]	CTE
low (-)	60	190	100	500	1	8,84220E+13	1500	850	400	0,00003
high (+)	100	230	150	1500	3	6,22000E+16	15000	7500	3750	0,00050

A1.4 Design of simulated experiments

In order to compare the simulated process with the real one, it was decided to build the simulation plan using the design of experiment approach by creating a fractional factor plan with 10 factors (Table A1.2) without replicas whose details are reported in Table A1.3.

Table A1.3 – Design summary of the design of simulation plan

Factors:	10	Base Design:	10; 128	Resolution:	V
Runs:	129	Replicates:	1	Fraction:	1/8
Blocks:	1	Center pts (total):	1		

Design Generators: H = ABCG; J = BCDE; K = ACDF

Block Generators: ADG

Defining Relation: I = ABCGH = BCDEJ = ACDFK = ADEGHJ = BDFGHK = ABFEJK = CEFGHJK

The response variable identified as useful for comparing simulation results with experimental results is the percentage error reported in eq. A1.3

$$\text{percentage error} = \left(\frac{\text{Experimental weigh} - \text{Simulated weight}}{\text{Experimental weight}} \right) * 100 \quad (\text{A1.3})$$

A1.5 Coding of experiments related to flash

In literature, the flash formation has been predicted in a single micropart production by adding the venting channel as part of the cavity domain [1, 2]. With the novel approach proposed in this section, the flash formation during the simulations has been associated with the overcoming of the clamping force. The limit value of the clamping force can be set in the simulator and when the process exceeds the limit, the software provides some warning messages, available in the real time log file on the screen, which do not inhibit the simulation itself.

In the following table A1.4 is reported the coding criteria adopted for the simulated experiments in order to differentiate the response behaviour in terms of weight and flash of the simulator from the experiments described in Chapter 4.

Table A1.4 – coding criteria for simulated experiments

FLASH			
Simulation	Experimentation	Condition	Available data

0	0	(0 0)	55 + 10 center points of experimental campaign
0	1	(0 1)	24
1	0	(1 0)	18
1	1	(1 1)	29 (+2)*

where:

0 = no flash; 1 = flash

*N.2 simulated experiments were not completed successfully but they gave a warning on the clamping force confirmed by the flash for experimental trials with same process parameters.

A1.6 Regression on condition (0 0)

A1.6.1 Full model

In the following section it is reported the analysis of variance (Table A1.5) related to the condition (0 0), which means that for both compared trials we have absence of flash. The analysis of variance evidenced a great significativity of the Phold and of Tmelt, as expected, and high significativity also of the HTC packing, a simulator parameter.

Table A1.5 – Analysis of variance for the full model related to the condition (0 0)

Source	DF	Adj SS	Adj MS	F-Value	P-Value
Regression	45	1921,28	42,695	24,11	0,000
Tmold	1	2,58	2,584	1,46	0,242
Tmelt	1	22,66	22,662	12,80	0,002
vinj	1	0,26	0,257	0,14	0,708
Phold	1	100,11	100,114	56,54	0,000
thold	1	0,07	0,069	0,04	0,846
D1	1	12,71	12,708	7,18	0,015
HTC filling	1	0,00	0,001	0,00	0,981
HTC packing	1	35,43	35,428	20,01	0,000
HTC detached	1	7,13	7,133	4,03	0,059
CTE alfa	1	6,62	6,617	3,74	0,068
Tmold*Tmold	1	25,15	25,148	14,20	0,001
Tmold*Tmelt	1	0,72	0,720	0,41	0,531
Tmold*vinj	1	1,19	1,194	0,67	0,422
Tmold*Phold	1	11,18	11,183	6,31	0,021
Tmold*thold	1	0,31	0,309	0,17	0,681
Tmold*D1	1	0,25	0,251	0,14	0,711
Tmold*HTC filling	1	0,12	0,121	0,07	0,796
Tmold*HTC packing	1	2,29	2,295	1,30	0,269
Tmold*HTC detached	1	0,08	0,078	0,04	0,836
Tmelt*vinj	1	1,85	1,847	1,04	0,320
Tmelt*Phold	1	11,59	11,595	6,55	0,019
Tmelt*thold	1	0,48	0,477	0,27	0,610
Tmelt*D1	1	0,00	0,002	0,00	0,971
Tmelt*HTC filling	1	0,00	0,000	0,00	0,987
Tmelt*HTC packing	1	0,00	0,002	0,00	0,971
Tmelt*HTC detached	1	1,26	1,261	0,71	0,409
Tmelt*CTE alfa	1	0,34	0,339	0,19	0,667
vinj*Phold	1	0,03	0,029	0,02	0,900
vinj*thold	1	12,09	12,088	6,83	0,017
vinj*D1	1	1,09	1,086	0,61	0,443
vinj*HTC detached	1	0,23	0,234	0,13	0,720
vinj*CTE alfa	1	2,69	2,691	1,52	0,233

Phold*thold	1	3,21	3,212	1,81	0,194
Phold*HTC filling	1	0,48	0,478	0,27	0,609
thold*D1	1	2,40	2,404	1,36	0,258
thold*HTC filling	1	0,41	0,414	0,23	0,634
thold*HTC packing	1	13,71	13,707	7,74	0,012
thold*CTE alfa	1	0,13	0,129	0,07	0,790
D1*HTC filling	1	0,04	0,035	0,02	0,889
D1*HTC packing	1	4,39	4,393	2,48	0,132
D1*HTC detached	1	1,26	1,259	0,71	0,410
HTC filling*HTC detached	1	1,95	1,953	1,10	0,307
HTC filling*CTE alfa	1	0,07	0,070	0,04	0,845
HTC packing*HTC detached	1	0,59	0,593	0,34	0,569
HTC detached*CTE alfa	1	0,03	0,028	0,02	0,901
Error	19	33,65	1,771		
Lack-of-Fit	10	20,03	2,003	1,32	0,342
Pure Error	9	13,62	1,513		
Total	64	1954,92			

Model Summary

S	R-sq	R-sq(adj)	R-sq(pred)
1,33072	98,28%	94,20%	*

A1.6.1 Reduced model for condition (0 0)

The reduced model confirmed the significance of the Phold compared to the other parameters (Table A1.6). The regression model identified (eq. A1.4) has an R^2_{adj} around 80%, so still with a good prediction capability. The normality plot in Fig. A1.1(left) evidenced a normal distribution of the residuals, while for the scatterplot of Fig. A1.1 (right) all the values are in the interval $[-3; +3]$ and there is no evidence of outliers.

Table A1.6 – Analysis of variance for the reduced model related to the condition (0 0)

Source	DF	Adj SS	Adj MS	F-Value	P-Value
Regression	5	1607,90	321,58	54,67	0,000
Tmold	1	14,43	14,43	2,45	0,123
Tmelt	1	27,48	27,48	4,67	0,035
Phold	1	1542,07	1542,07	262,17	0,000
HTC packing	1	102,60	102,60	17,44	0,000
Tmold*Tmold	1	243,65	243,65	41,42	0,000
Error	59	347,03	5,88		
Lack-of-Fit	50	333,41	6,67	4,41	0,011
Pure Error	9	13,62	1,51		
Total	64	1954,92			

Model Summary

S	R-sq	R-sq(adj)	R-sq(pred)
2,42525	82,25%	80,74%	78,21%

Regression Equation

$$\text{Perc. error} = 0,870 + 0,568 \text{ Tmold} + 0,718 \text{ Tmelt} + 6,957 \text{ Phold} - 1,442 \text{ HTC packing} + 5,753 \text{ Tmold*Tmold} \quad (\text{A1.4})$$

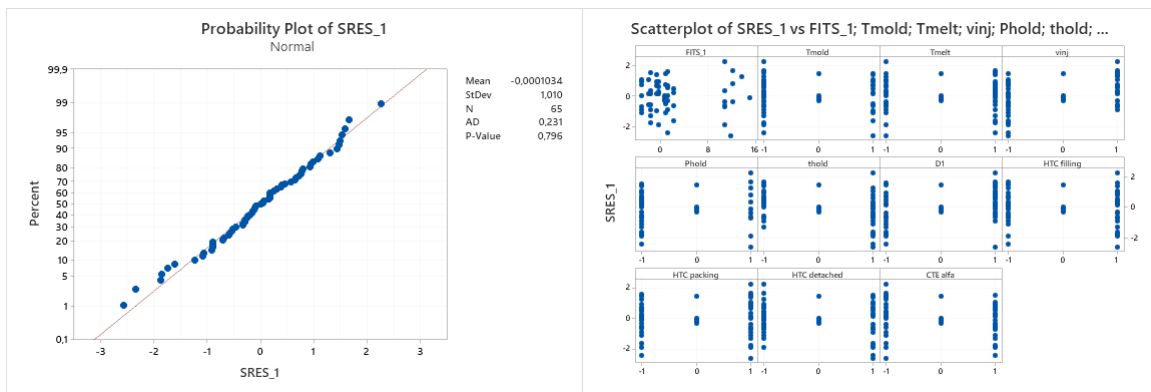


Fig. A1.1 – normality distribution (left) and scatterplot of standard residuals versus fits and process parameters (right) for condition (0 0)

A1.7 Regression analysis on condition (0 0) + (1 0)

A deeper analysis of the clamping force results concerning the condition (1 0), so flash detected for simulation but not confirmed by experimentaiton, showed that more than half of the simulated trials of the condition (1 0) didn't exceed too much the limit of the clamping force (Fig. A1.2).

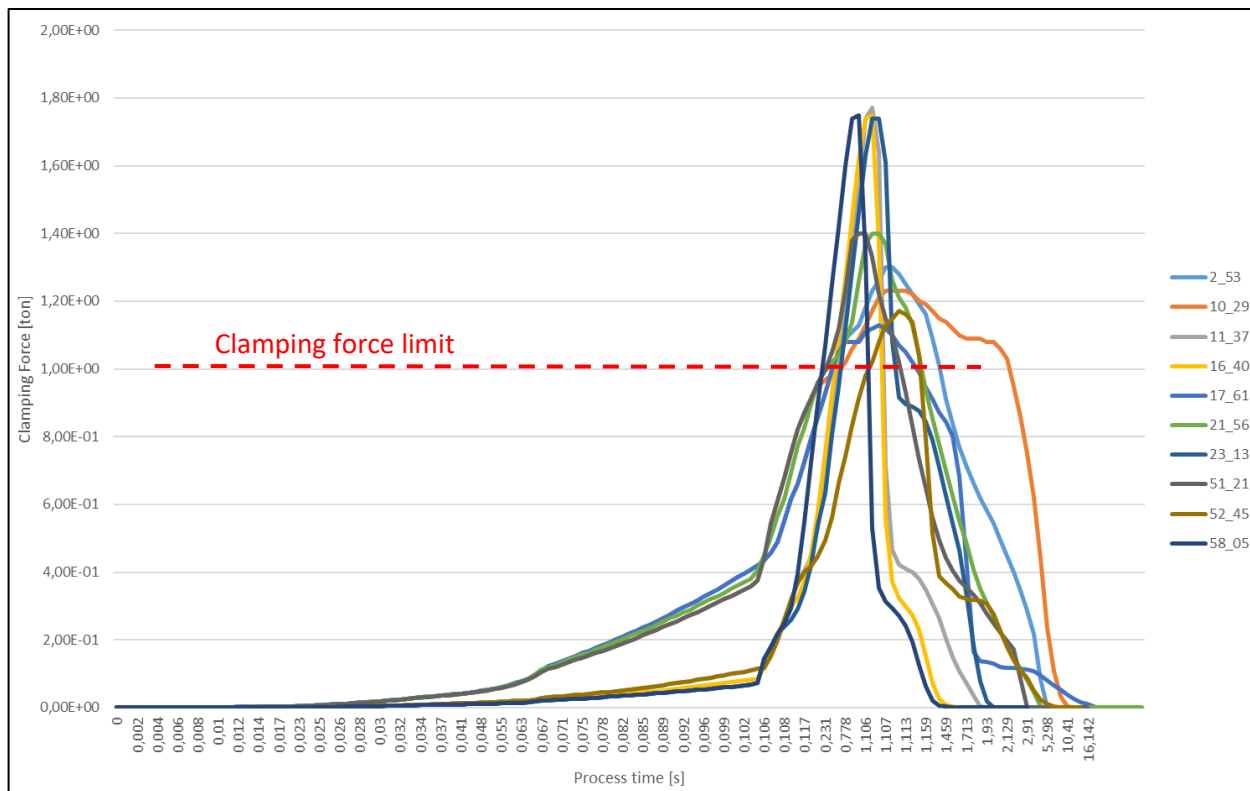


Fig. A1.2 – Clamping force distribution for trials related to the condition (1 0)

The analysis of variance (Table A1.7) confirmed the significance of the parameters identified with the condition (0 0) but with the addition also of D1 but with low impact on the process.

Table A1.7 – Analysis of variance for the full model related to the condition (0 0) + (1 0)

Source	DF	Adj SS	Adj MS	F-Value	P-Value
Regression	48	3240,87	67,518	42,97	0,000
Tmold	1	2,39	2,389	1,52	0,226
Tmelt	1	48,19	48,187	30,66	0,000
vinj	1	8,04	8,041	5,12	0,030
Phold	1	812,79	812,789	517,23	0,000
thold	1	2,76	2,757	1,75	0,194
D1	1	21,03	21,033	13,38	0,001
HTC filling	1	4,20	4,200	2,67	0,111
HTC packing	1	53,62	53,624	34,12	0,000
HTC detached	1	5,90	5,899	3,75	0,061
CTE alfa	1	5,76	5,762	3,67	0,064
Tmold*Tmold	1	123,27	123,266	78,44	0,000
Tmold*Tmelt	1	0,31	0,310	0,20	0,660
Tmold*vinj	1	0,02	0,019	0,01	0,914
Tmold*Phold	1	9,16	9,158	5,83	0,021
Tmold*thold	1	0,44	0,441	0,28	0,600
Tmold*D1	1	6,37	6,373	4,06	0,052
Tmold*HTC filling	1	2,01	2,013	1,28	0,266
Tmold*HTC packing	1	1,98	1,977	1,26	0,270
Tmold*HTC detached	1	0,66	0,660	0,42	0,521
Tmold*CTE alfa	1	0,01	0,013	0,01	0,929
Tmelt*vinj	1	1,91	1,914	1,22	0,278
Tmelt*Phold	1	26,38	26,382	16,79	0,000
Tmelt*thold	1	0,00	0,000	0,00	0,992
Tmelt*D1	1	0,05	0,047	0,03	0,864
Tmelt*HTC filling	1	1,08	1,081	0,69	0,413
Tmelt*HTC packing	1	2,08	2,082	1,33	0,258
Tmelt*HTC detached	1	2,75	2,746	1,75	0,195
Tmelt*CTE alfa	1	0,27	0,270	0,17	0,681
vinj*Phold	1	3,73	3,735	2,38	0,132
vinj*thold	1	21,16	21,159	13,46	0,001
vinj*D1	1	1,80	1,800	1,15	0,292
vinj*HTC detached	1	4,03	4,025	2,56	0,119
vinj*CTE alfa	1	15,45	15,448	9,83	0,004
Phold*thold	1	7,45	7,453	4,74	0,036
Phold*HTC filling	1	0,23	0,228	0,14	0,706
Phold*HTC packing	1	0,31	0,310	0,20	0,660
thold*D1	1	6,09	6,089	3,87	0,057
thold*HTC filling	1	0,19	0,187	0,12	0,732
thold*HTC packing	1	30,53	30,534	19,43	0,000
thold*CTE alfa	1	0,14	0,145	0,09	0,763
D1*HTC filling	1	4,22	4,215	2,68	0,111
D1*HTC packing	1	6,46	6,458	4,11	0,051
D1*HTC detached	1	0,15	0,146	0,09	0,762
HTC filling*HTC detached	1	0,01	0,006	0,00	0,949
HTC filling*CTE alfa	1	1,76	1,757	1,12	0,298
HTC packing*HTC detached	1	0,03	0,026	0,02	0,899
HTC packing*CTE alfa	1	0,02	0,023	0,01	0,905
HTC detached*CTE alfa	1	0,50	0,497	0,32	0,578
Error	34	53,43	1,571		
Lack-of-Fit	25	39,81	1,592	1,05	0,499
Pure Error	9	13,62	1,513		
Total	82	3294,30			

Model Summary

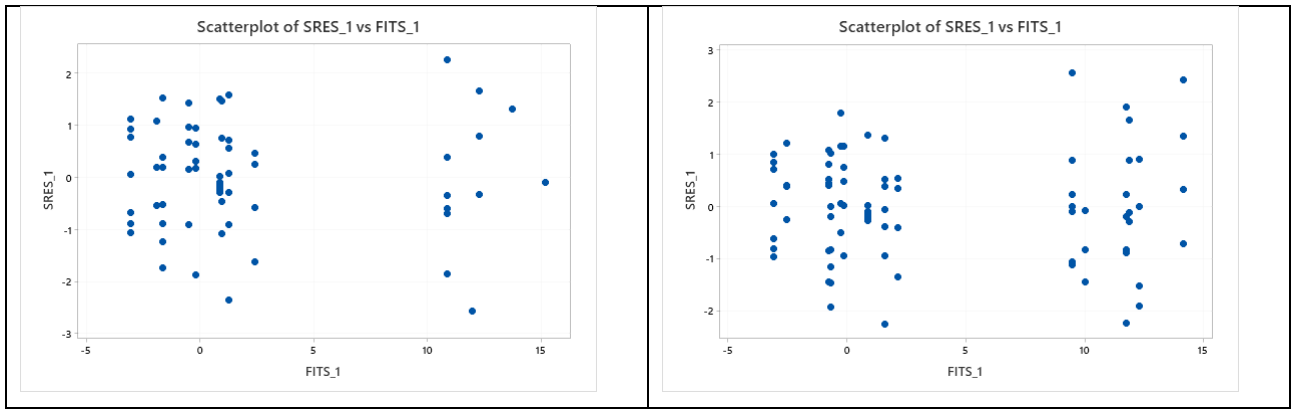
S	R-sq	R-sq(adj)	R-sq(pred)
1,25357	98,38%	96,09%	*

A1.8 Comparison of reduced models

The comparison between the regression analysis for the condition (0 0) and the one extended to condition (0 0) + (1 0), shows that the models found have very similar coefficients (Table A1.8). If we analyze the R2adj we can detect a minimum improvement for the model obtained from the conditions (0 0) + (1 0) compared to the one of condition (0 0). However the error increases slightly for the condition (0 0) + (1 0). Therefore the models are both valid and this allows us, with the model obtained from the condition (0 0) + (1 0), to be able to monitor an eligible region wider than the one with condition (0 0).

Table A1.8 – Synthesis of regression analysis for reduced models of condition (0 0) and (0 0)+(1 0)

(0 0) reduced model						(0 0) + (1 0) reduced model					
Analysis of Variance						Analysis of Variance					
Source	DF	Adj SS	Adj MS	F-Value	P-Value	Source	DF	Adj SS	Adj MS	F-Value	P-Value
Regression	5	1607,90	321,58	54,67	0,000	Regression	5	2748,70	549,74	77,58	0,000
Tmold	1	14,43	14,43	2,45	0,123	Tmold	1	4,36	4,36	0,62	0,435
Tmelt	1	27,48	27,48	4,67	0,035	Tmelt	1	95,24	95,24	13,44	0,000
Phold	1	1542,07	1542,07	262,17	0,000	Phold	1	2522,63	2522,63	356,02	0,000
HTC packing	1	102,60	102,60	17,44	0,000	HTC packing	1	94,48	94,48	13,33	0,000
Tmold*Tmold	1	243,65	243,65	41,42	0,000	Tmold*Tmold	1	206,44	206,44	29,13	0,000
Error	59	347,03	5,88			Error	77	545,60	7,09		
Lack-of-Fit	50	333,41	6,67	4,41	0,011	Lack-of-Fit	68	531,98	7,82	5,17	0,006
Pure Error	9	13,62	1,51			Pure Error	9	13,62	1,51		
Total	64	1954,92				Total	82	3294,30			
Model Summary						Model Summary					
S	R-sq	R-sq(adj)	R-sq(pred)			S	R-sq	R-sq(adj)	R-sq(pred)		
2,42525	82,25%	80,74%	78,21%			2,66189	83,44%	82,36%	80,88%		
Regression Equation						Regression Equation					
percentage = 0,870 + 0,568 Tmold + 0,718 Tmelt error + 6,957 Phold - 1,442 HTC packing + 5,753 Tmold*Tmold						percentage = 0,870 + 0,264 Tmold + 1,191 Tmelt error + 6,272 Phold - 1,138 HTC packing + 4,926 Tmold*Tmold					



A1.9 Conclusions

In this appendix are reported the results of a preliminary comparative analysis between simulation and testing of the micro injection moulding process. The aim was to assess the simulator's ability to predict the real behavior of the process.

The simulation investigation was performed using the same DoE plan used for the experiments, obviously without replicas because the simulator is deterministic, in order to directly compare the results. The innovative aspect compared to the state of the art was to include in the simulation plan, in addition to the process parameters used for testing, some parameters of the simulator that are HTC (heat transfer coefficient), the parameter D1 of the Cross-WLF viscosity model and the coefficient of thermal expansion (α).

A criterion able to associate the flash constraint to a simulation result has been identified, that is considering, as a simulation event that generates the flash, a warning that advises about the overcoming of the clamping force.

From a first direct comparative analysis between simulation and experimental results, it was found that the simulator was able to predict as well as the experimentation in 67.5% of cases compared, of which about 43,5% the absence of flash and about 24% the presence of flash.

The response variable identified as useful for comparing simulation results with experimental results is the percentage error with which the simulator is wrong compared to the experiments.

In this preliminary phase it has been identified a regression model with which it is possible to predict in a rather reliable way the set of parameters that can minimize the percentage error in absence of flash.

Future developments foresee further investigations on the model identified with the aim of being able to build a confidence region of the deterministic optimal thanks to the stochastic part due to the experimentation.

The study has also shown that only a couple of parameters of the simulator have proved to be influential on the weight, and it will be interesting to extend this type of approach to other observation variables, such as shrinkage, to assess which simulator parameters affect the new variable as well as considering other defects typical of the micro injection moulding process, such as warpage.

A1.10 References

- [1] Loaldi, D.; Regi, F.; Baruffi, F.; Calaon, M.; Quagliotti, D.; Zhang, Y.; Tosello, G. (2020), Experimental Validation of Injection Molding Simulations of 3D Microparts and Microstructured Components Using Virtual Design of Experiments and Multi-Scale Modeling, *Micromachines*, 11, 614;
- [2] Baruffi, F. (2019) 'Integrated micro product/process quality assurance in micro injection moulding production', PhD thesis, Technical University of Denmark, Department of Mechanical Engineering, (<https://orbit.dtu.dk/en/publications/integrated-micro-productprocess-quality-assurance-in-micro-inject>).

